Advances in Nano Research, *Vol. 11, No. 1 (2021) 83-99*
https://doi.org/10.12989/anr.2021.11.1.083

Computer simulation for stability performance of sandwich annular system via adaptive tuned deep learning neural network optimization

Yan Ming[1], Yousef Zandi*[2], Morteza Gholizadeh[2], Khaled Oslub[3], Mohamed Amine Khadimallah[4,5] and Alibek Issakhov[6,7]

[1]*School of Mechatronic Engineering and Automation, Shanghai University, Shanghai 200444, China*
[2]*Department of Civil Engineering, Tabriz Branch, Islamic Azad University, Tabriz, Iran*
[3]*Faculty of Mechanical Engineering, Tabriz University, Tabriz, Iran*
[4]*Prince Sattam Bin Abdulaziz University, College of Engineering, Civil Engineering Department, Al-Kharj, 16273, Saudi Arabia*
[5]*Laboratory of Systems and Applied Mechanics, Polytechnic School of Tunisia, University of Carthage, Tunis, Tunisia*
[6]*Al-Farabi Kazakh National University, Almaty, Kazakhstan*
[7]*Kazakh-British Technical University, Almaty, Kazakhstan*

(*Received November 14, 2020, Revised April 30, 2021, Accepted June 24, 2021*)

Abstract. In this article with the aid of adaptively tuned deep neural network (DNN), dynamic stability analysis of the sandwich structure has been investigated. Due to finding the design-points features, the numerical solution procedure called two-dimensional generalized differential quadrature technique has been applied to the ordinary differential equations of the current structure system acquired on the foundation of the kinematic theory with refined higher order terms. Also, the involved parameters with the optimum values in the fully-connected neural network mechanism are obtained via momentum-based optimizer. For modeling a moderately thick structure, higher order terms of shear deformation are chosen. For stability analysis of the current structure the design points considering the method of adaptive learning is presented. For analysis of the current structure 'accuracy (used for determining the design-points) is presented through than the published outcomes in the literature. The outcomes of accuracy section of the current research show that the DNN-based model in analysis of the sandwich structure has less error than other models. The results show that the current momentum-based optimizer can be good tool for future researches about stability analysis of the various structure due to its good accuracy.

Keywords: DNN, GDQM, honeycomb core, frequency characteristic, sandwich disk

1. Introduction

As a rely of fact, further to enhancing the thermomechanical reaction of the applicable systems with the beneficial useful resource of using the sandwich systems, within side the very last decant, researches positioned a completely unique and exceptional method for reinforcing the dynamic and static information of the low-density disk, plate, shell, and beam (Ma *et al*. 2021, Zhao *et al*. 2021, Huang *et al*. 2021). This kind of structure can be used in many structures such as (Zhang *et al*. 2018, 2019, 2020c, Shi *et al*. 2019). Primarily according to the totally mostly on this rely, structures called honeycomb are provided for use in the associated corporation (Huang *et al*. 2021, Jiao *et al*. 2021, Moradi *et al*. 2021). Mukhopadhyay *et al*. (2016) investigated frequency information of the sandwich shell structure with lattice core and composite face sheets with the useful resource called Hamilton's principle. In this research they found that the honeycomb structure has marvelous impact on the frequency information of their composite structure. This kind of materials can be used in many applications such as (Gong *et al*. 2019, Li *et al*. 2020, 2021a, Zhang *et al*. 2021)

Also, one of their important outcomes was that the geometry of the honeycomb core should be selected with the high accuracy. This was because, in some angle ply of honeycomb core, the structure encounters the instability in response. Ref. (Suryawanshi *et al*. 2020) investigated the impacts of different shape of honeycomb core, and influence of this shape on the mechanical performance of the lattice beams in various conditions via series Fourier, as well as finite element method. Also, one of their important outcomes was that the geometry of the honeycomb core should be selected with the high accuracy. The frequency performance of the lattice core system via Hamilton's principle as well as Navier solution procedure for solving the motion equations was conducted by Ref. (Xu *et al*. 2019). In this study they showed that solution procedure and acquired frequency have linear behavior with each other. Also, other important consequence was that geometry of the honeycomb core have important role on the mechanical performance of the lattice core system (Ghabussi *et al*. 2019, 2020, Safarpour *et al*. 2020, Shariati *et al*. 2020a). In recent years, in addition to the experimental and numerical techniques (Arabnejad Khanouki *et al*. 2011, Jalali *et al*. 2012), artificial intelligence (AI) algorithms have been developed and employed in various fields, especially civil engineering

*Corresponding author, Ph.D.,
E-mail: zandi@iaut.ac.ir

ISSN: 2287-237X (Print), 2287-2388 (Online)

(Shariati *et al*. 2017, Safa *et al*. 2020,). In fact, AI is able to accurately optimize and predict the experimental data. Researchers have developed several sub-sets of AI algorithms such as ANFIS, PSO, machine learning and hybrid algorithms like PSO-ELM, ANFIS-PSO (Naghipour *et al*. 2020, Razavian *et al*. 2020, Shariati 2020). The advantages of AI models compared to experimental methods are high accuracy and cost-effectiveness. Also, they require lower time to process the data than other numerical approaches (Shariati *et al*. 2010, 2019 Hamidian *et al*. 2011, Mohammadhassani *et al*. 2014, Nasrollahi *et al*. 2018). The mentioned solution procedure as a strong solver can be used in many systems such as (Xu *et al*. 2020, Xue *et al*. 2020, Ma *et al*. 2021, Zhang *et al*. 2021b).

Amini *et al*. (2019) presented a novel aspect of vibration analysis called frequency control of the solar shell made of lattice core and piezoelectric face-sheets. Higher order shear deformation theory as well as Hamilton's principle were used for obtaining the electrically motion equations of their structure. Consequently, they showed that the applied voltage of the structure and frequency performance of the smart systems have linear behavior with each other. Ref. (Shahverdi *et al*. 2019) presented the nonlinear instability analysis of the shells with nanocomposite face-sheets and lattice core. Their findings demonstrated that GPL's weight fraction, as well as geometric properties of the honeycomb core has linear behavior with the nonlinear instability performance of the shells with nanocomposite face-sheets and lattice core. The bending performance of the beam with deep curvature, lattice core, and functionally graded layers was conducted by Sobhy (Sobhy 2020). The previous solution procedure can be used in many systems (Jiang *et al*. 2021, Li *et al*. 2021, Lou *et al*. 2021, Yu *et al*. 2021). Also, owing to new demand in technology (Lou *et al*. 2021, Lv *et al*. 2021a, b, c), the previous solution procedure is a strong tool for solving various complex structures. With the aid of numerical solution called DQM their graded motion equations and boundary edges was solved. One of their important consequence was that functionally graded materials and frequency of a composite structure have linear behavior with each other. Also, this kind of analysis can be used in many systems (Zuo *et al*. 2015, 2017, Zhang *et al*. 2020a, Zaher *et al*. 2020). Wang *et al*. (2019) presented a novel research about dynamic stability performance of the multi-layer system with lattice core via finite element and experimental tests. In this important research they showed that experimental data and dynamic stability of a structure have linear behavior with each other. Also, other important consequence was that all designers should have attention to the angle ply of the lattice core. This kind of analysis can be used in many structures and systems such as (Cao *et al*. 2019, Dorri *et al*. 2019, Libo *et al*. 2019, Puri *et al*. 2019, Tang *et al*. 2019). Ref. (Zhang *et al*. 2017) conducted a research about dynamic stability analysis of the multi-layer beam made of lattice core via finite element and experimental tests. In this important research they showed that experimental data and dynamic stability of a multi-layer structure have linear behavior with each other. As well as this, the optimization algorithm method can be a good tool for solving the complex structures and systems (Eassa *et al*. 2018, Hurrah *et al*. 2019, Muhammad *et al*. 2019, Murugan *et al*. 2019, Valayapalayam Kittusamy *et al*. 2019). On the nonlinear dynamics (Gaber *et al*. 2018, Yuan *et al*. 2018) of the lattice multi-layer structure via multiple scales method was conducted by Zhang *et al*. (2019). In their important article they showed that solution procedure has important role on the finding of nonlinear frequency of a system. The presented approach in the previous reference can be a good tool for analysis of complex systems (Zhou *et al*. 2019, 2020, 2021). Because of some advantage of GPLs, this sort of reinforcement has been given several interest within the beyond few years. loose vibration assessment of a GPLRC plate with the useful resource of a numerical answer method changed into presented via way of Gunasekaran *et al*. (2020). Due to new demand in technology composite structures can be used as the main materials in the future (Yang *et al*. 2019, Hu *et al*. 2020, Qu *et al*. 2021, Zhang *et al*. 2021d). The presented approach in the previous reference can be a good tool for analysis of complex systems (Elhoseny *et al*. 2014, Metawa *et al*. 2016, Abd El Aziz *et al*. 2017, Tharwat *et al*. 2018, Devaraj *et al*. 2020). With the useful resource of FEM, compelled vibration traits of a GPLRC curved plate excessive-temperature environment turned into furnished by way of Ref. (Tran *et al*. 2020). One of the crucial consequences that they showed in their paintings modified into that the geometrical homes of the GPLs have an essential have an impact at the resonance conduct of the GPLRC curved structure. currently, the important temperature of a composite annular location plate via way of the usage of considering von kármán nonlinearity and primary-order shear deformation idea turn out to be furnished thru Javani *et al*. (2020). The used method of previous reference can be a good tool for solving the complex problems such as (Abdel-Basset *et al*. 2019, Elhoseny *et al*. 2019, Lakshmanaprabu *et al*. 2019, Krishnaraj *et al*. 2020, Zaher *et al*. 2020). Some researchers used computer modeling for analysis of various systems (Elhoseny *et al*. 2017, Elsayed *et al*. 2018, Rizk-Allah *et al*. 2018, Hosseinabadi *et al*. 2019, Mohanty *et al*. 2020, Krishnaraj *et al*. 2021). They used generalized differential quadrature method for obtaining the exact thermal buckling responses of the GPLRC curved structure. Due to several static and dynamic loads that may cave in the stability of the machine, the furnished shape is frequently underneath complicated conditions. except, undesirable behaviors may also moreover rise up for the ones systems, at the side of buckling, deformations, and resonance (Bai *et al*. 2020). So, it's miles very vital to apprehend the fashion dressmaker about the mechanical behavior of this sort of machine to research the cited shape with the immoderate guarantee reliability. regular with the benefit of the GRLs reinforcement, this sort of material can be used as a composite reinforcement in the annular plates. Bending and frequency performance of the composite annular plate via 3D-elasticity theory as the best continuum- based theory was examined by Liu *et al* (2019). They showed that the radius ratio of the composite annular system has important role on the bending and frequency information of the mentioned structure. The presented approach in the previous reference can be a good tool for analysis of

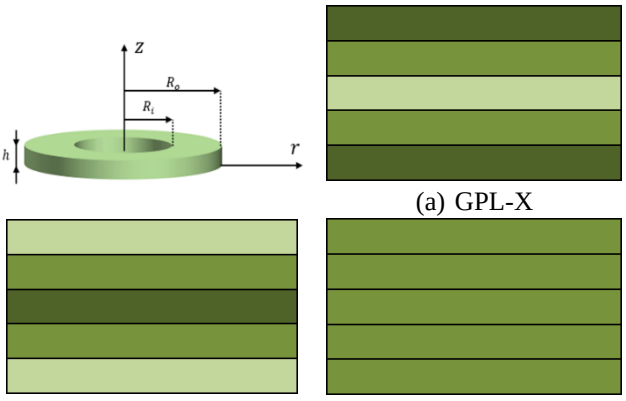

(a) GPL-X

(b) GPL-O (c) GPL-UD

Fig. 1 A schematic diagram of a sandwich disk

medical problems (Abdel-Basset *et al*. 2019, Elhoseny *et al*. 2019b, Elhoseny and Shankar 2019, Shankar *et al*. 2019, Thakur *et al*. 2019, Dutta *et al*. 2020). Using optimization algorithm can solve the complex equations (Ewees *et al*. 2017, Elhoseny *et al*. 2018, Shankar *et al*. 2020, Xu *et al*. 2020). Wang *et al*. (2020) presented a novel research about the stability analysis of the composite structure in thermal situation via a numerical solution procedure. In this research they showed that the solution procedure for obtaining the real results of the system has linear communication with each other. In addition, this kind of analysis can be used in advance structures (Morasaei *et al*., Al-Furjan *et al*. 2020, Ghabussi *et al*. 2020, 2021). Computer simulation is a strong tool for modeling a structure (Abdel-Basset *et al*. 2020, Ali *et al*. 2020, El-Hasnony *et al*. 2020, Saračević *et al*. 2020, Uthayakumar *et al*. 2020). Also, recently, some researchers did study for finding the stability regions of various nanostructures (Tounsi *et al*. 2013, Salari 2016, Ebrahimi *et al*. 2019, 2020, Ghannadpour *et al*. 2019). In this article with the aid of adaptively tuned deep neural network (DNN), dynamic stability analysis of the sandwich structure has been investigated. Due to finding the design-points features, the numerical solution procedure called two-dimensional generalized differential quadrature technique has been applied to the ordinary differential equations of the current structure system acquired on the foundation of the kinematic theory with refined higher order terms. Also, the involved parameters with the optimum values in the fully-connected neural network mechanism are obtained via momentum-based optimizer. For modeling a moderately thick structure, higher order terms of shear deformation are chosen. For stability analysis of the current structure the design points considering the method of adaptive learning is presented. For analysis of the current structure 'accuracy (used for determining the design-points) is presented through than the published outcomes in the literature. The outcomes of the current report show that radius curvature, composite patterns, angle of hexagonal middle, the thickness of compositionally layers, and geometry of the lattice core have an essential function within side the frequency traits of a sandwich annular system with lattice middle and compositionally layers.

2. The mathematical formulations for sandwich disk with honeycomb core

In this paper, we focused on the dynamics of a sandwich disk with honeycomb core as is shown in Fig. 1. Also, it is well known that in the manufacturing process, the structures will encounter residual stress due to some reason, so, in the present computational approach, we consider residual stress as an internal pressure in the sandwich disk. Besides, the formulation of the mentioned issue is presented in the following sections.

According to the Halpin-Tsai micromechanics model, have

$$\breve{E} = -\breve{E}_M \times \left(\frac{3+3V_{GPL}\eta_L\xi_L}{8V_{GPL}\eta_L - 8} - \frac{5+5V_{GPL}\eta_W\xi_W}{8V_{GPL}\eta_W - 8} \right)$$

$$\breve{\xi}_L = 2\frac{l_{GPL}}{t_{GPL}}, \quad \breve{\xi}_W = 2\frac{w_{GPL}}{t_{GPL}}, \quad \breve{\mathrm{V}}^{\bullet}_{GPL} = \frac{\Lambda_{GPL}}{\left(\frac{\breve{\rho}_{GPL}}{\breve{\rho}_M} - \frac{\Lambda_{GPL}\breve{\rho}_{GPL}}{\breve{\rho}_M} \right) + \Lambda_{GPL}} \quad (1)$$

$$\breve{\eta}_W = -\frac{\frac{\breve{E}_M}{\breve{E}_{GPL}} - 1}{\frac{\breve{\xi}_W \breve{E}_M}{\breve{E}_{GPL}} + 1}, \quad \breve{\eta}_L = \frac{1 - \frac{\breve{E}_M}{\breve{E}_{GPL}}}{1 + \frac{\breve{\xi}_L \breve{E}_M}{\breve{E}_{GPL}}}$$

The effective Poisson's ratio, mass density, and thermal expansion coefficient based on role of mixture can be formulated as below

$$\begin{aligned} \breve{\rho} &= \breve{\rho}_{GPL}\breve{V}_{GPL} + \breve{\rho}_M\left(1 - \breve{V}_{GPL}\right) \\ \breve{\nu} &= \breve{\nu}_{GPL}\breve{V}_{GPL} + \breve{\nu}_M\left(1 - \breve{V}_{GPL}\right) \\ \breve{\alpha} &= \breve{\alpha}_{GPL}\breve{V}_{GPL} + \breve{\alpha}_m\left(1 - \breve{V}_{GPL}\right) \end{aligned} \quad (2)$$

Also, for effective shear modulus have:

$$\breve{G} = \frac{\breve{E}}{2\left(1 + \breve{\nu}\right)} \quad (3)$$

Finally, various kinds of GPL distribution along with thickness direction can be given as follows:

$$\breve{\mathrm{V}}^{\bullet}_{GPL}\left(\breve{z}_j\right) = \begin{cases} 2 \times V^{\bullet}_{GPL} \times \dfrac{2\left|\breve{z}_j\right|}{h} & \mathrm{GPL}-X \\ 2 \times V^{\bullet}_{GPL} \times \left(1 - 2\dfrac{\left|\breve{z}_j\right|}{h}\right) & \mathrm{GPL}-O \\ V^{\bullet}_{GPL} & \mathrm{GPL}-UD \end{cases} \quad (4)$$

$$\breve{z}_j = h \times \left(0.5 + \frac{0.5}{n} - \frac{q}{n}\right), \quad q = 1, 2, 3, \ldots, n$$

2.1 Honeycomb core modelling

The hexagonal cell geometry has been illustrated in Fig. 2. According to the Gibson model, have (Gibson *et al*. 1999):

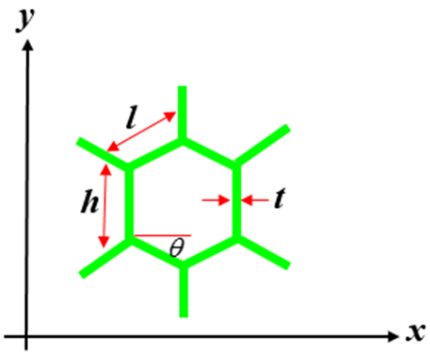

(c)

Fig. 2 The hexagonal cell geometry

$$\breve{E}_{11}^{*}=\frac{\breve{\sigma}_1}{\breve{\varepsilon}_1}=\breve{E}_S A\times\frac{\beta}{(B+\alpha)\alpha^2}\times\frac{1}{1+A^2\dfrac{\beta^2}{\alpha^2}} \tag{5a}$$

$$\breve{E}_{22}^{*}=\frac{\breve{\sigma}_2}{\breve{\varepsilon}_2}=\breve{E}_S A^3\times\frac{(B+\alpha)}{\beta^3}\times\frac{1}{1+A^2\dfrac{\beta^2}{\alpha^2}} \tag{5b}$$

$$\breve{\nu}_{12}^{*}=-\frac{\breve{\varepsilon}_2}{\breve{\varepsilon}_1}=\frac{\beta^2}{(B+\alpha)\alpha}\times\frac{1-A^2}{1+\dfrac{\beta^2}{\alpha^2}A^2} \tag{5c}$$

$$\breve{\nu}_{21}^{*}=-\frac{\breve{\varepsilon}_1}{\breve{\varepsilon}_2}=\frac{(B+\alpha)\alpha}{\beta^2}\times\frac{1-A^2}{1+\left(B\dfrac{1}{\alpha^2}+\dfrac{\alpha^2}{\beta^2}\right)A^2} \tag{5d}$$

$$\breve{G}_{12}^{*}=\breve{E}_S\times A^3\times\frac{(B+\alpha)}{(h/l)^2\beta}\times\frac{1}{\breve{R}} \tag{5e}$$

$$\breve{R}=\left(1+2\times B+A^2\frac{(B+\alpha)}{B^2}\left[(B+\alpha)\frac{\alpha^2}{\beta^2}+\alpha\right]\right) \tag{5f}$$

$$\frac{\rho^{*}}{\rho_S}=\frac{A(B+2)}{2\beta(B+\alpha)} \tag{5g}$$

where $A=\frac{t}{L}$, $B=\frac{h}{L}$, $\alpha=sin(\theta)$, and $\beta=cos(\theta)$.

2.2 Displacement fields

According to the FSDT, the fields of displacement can be defined as below:

$$\begin{aligned}\breve{u}^{\eta}&=\breve{u}_0^{\eta}+z\breve{u}_1^{\eta}\\ \breve{v}^{\eta}&=\breve{v}_0^{\eta}+z\breve{v}_1^{\eta}\\ \breve{w}^{\eta}&=\breve{w}_0^{\eta}\end{aligned} \tag{6}$$

In Eq. (6), defines the core, top, and bottom, layers.

2.3 Strain-stress of the honeycomb core

According to the FSDT, the strain- stress relations are (Ma *et al*. 2021, Zhang *et al*. 2021):

$$\begin{bmatrix}\breve{\sigma}_{RR}\\ \breve{\sigma}_{\theta\theta}\\ \breve{\sigma}_{R\theta}\\ \breve{\sigma}_{Rz}\\ \breve{\sigma}_{\theta z}\end{bmatrix}^{c}=\begin{bmatrix}\breve{Q}_{11} & \breve{Q}_{12} & 0 & 0 & 0\\ \breve{Q}_{12} & \breve{Q}_{22} & 0 & 0 & 0\\ & & \breve{Q}_{66} & 0 & 0\\ & sym. & & \breve{Q}_{55} & 0\\ & & & 0 & \breve{Q}_{44}\end{bmatrix}^{c}\begin{bmatrix}\breve{\varepsilon}_{RR}\\ \breve{\varepsilon}_{\theta\theta}\\ \breve{\varepsilon}_{R\theta}\\ \breve{\varepsilon}_{Rz}\\ \breve{\varepsilon}_{\theta z}\end{bmatrix}^{c} \tag{7}$$

$$\breve{Q}_{11}{}^{c}=\frac{\breve{E}_{11}^{*}}{1-\breve{\nu}_{12}^{*}\breve{\nu}_{21}^{*}},\ \breve{Q}_{22}{}^{c}=\frac{\breve{E}_{22}^{*}}{1-\breve{\nu}_{12}^{*}\breve{\nu}_{21}^{*}},\ \breve{Q}_{12}{}^{c}=\frac{\breve{\nu}_{21}^{*}\breve{E}_{22}^{*}}{1-\breve{\nu}_{12}^{*}\breve{\nu}_{21}^{*}},$$
$$\breve{Q}_{44}{}^{c}=\breve{G}_{12}^{*},\ \breve{Q}_{55}{}^{c}=\breve{G}_{13}^{*},\ \breve{Q}_{66}{}^{c}=\breve{G}_{23}^{*},\ \breve{G}_{13}^{*}=\breve{G}_{23}^{*}=\breve{G}_{12}^{*}$$

So, the strain components would be written as:

$$\begin{Bmatrix}\breve{\varepsilon}_{RR}\\ \breve{\varepsilon}_{\theta\theta}\\ \breve{\gamma}_{R\theta}\\ \breve{\gamma}_{Rz}\\ \breve{\gamma}_{\theta z}\end{Bmatrix}^{c}=\begin{bmatrix}\dfrac{\partial\breve{u}}{\partial R}\\ \dfrac{\partial\breve{v}}{R\partial\theta}+\dfrac{\breve{u}}{R}\\ \dfrac{\partial\breve{v}}{\partial R}+\dfrac{1}{R}\dfrac{\partial\breve{u}}{\partial\theta}-\dfrac{1}{R}\breve{v}\\ \dfrac{\partial\breve{u}}{\partial z}+\dfrac{\partial\breve{w}}{\partial R}\\ \dfrac{\partial\breve{v}}{\partial z}+\dfrac{1}{R}\dfrac{\partial\breve{w}}{\partial\theta}\end{bmatrix}^{c} \tag{8}$$

The stress-strain relations for FG-GPLRC face sheet layer are as below:

$$\begin{bmatrix}\breve{\sigma}_{RR}\\ \breve{\sigma}_{\theta\theta}\\ \breve{\sigma}_{R\theta}\\ \breve{\sigma}_{Rz}\\ \breve{\sigma}_{\theta z}\end{bmatrix}^{\psi}=\begin{bmatrix}\breve{Q}_{11} & \breve{Q}_{12} & 0 & 0 & 0\\ \breve{Q}_{12} & \breve{Q}_{22} & 0 & 0 & 0\\ & & \breve{Q}_{66} & 0 & 0\\ & sym. & & \breve{Q}_{55} & 0\\ & & & 0 & \breve{Q}_{44}\end{bmatrix}^{\psi}\begin{bmatrix}\breve{\varepsilon}_{RR}\\ \breve{\varepsilon}_{\theta\theta}\\ \breve{\varepsilon}_{R\theta}\\ \breve{\varepsilon}_{Rz}\\ \breve{\varepsilon}_{\theta z}\end{bmatrix}^{\psi} \tag{9}$$

$$\breve{Q}_{11}{}^{\psi}=\breve{Q}_{22}{}^{\psi}=\frac{\breve{E}}{1-\breve{\nu}^2},\ \breve{Q}_{12}{}^{\psi}=\frac{\breve{\nu}\breve{E}}{1-\breve{\nu}^2},\quad \breve{Q}_{44}{}^{\psi}=\breve{Q}_{55}{}^{\psi}=\breve{Q}_{66}{}^{\psi}=\breve{G}_{12}$$

In the above equation ψ defines the top and bottom layers. So, the strain components of the face sheet layers can be given by:

$$\begin{Bmatrix}\breve{\varepsilon}_{RR}\\ \breve{\varepsilon}_{\theta\theta}\\ \breve{\gamma}_{R\theta}\\ \breve{\gamma}_{Rz}\\ \breve{\gamma}_{\theta z}\end{Bmatrix}^{\psi}=\begin{bmatrix}\dfrac{\partial\breve{u}}{\partial R}\\ \dfrac{\partial\breve{v}}{R\partial\theta}+\dfrac{\breve{u}}{R}\\ \dfrac{\partial\breve{v}}{\partial R}+\dfrac{1}{R}\dfrac{\partial\breve{u}}{\partial\theta}-\dfrac{1}{R}\breve{v}\\ \dfrac{\partial\breve{u}}{\partial z}+\dfrac{\partial\breve{w}}{\partial R}\\ \dfrac{\partial\breve{v}}{\partial z}+\dfrac{1}{R}\dfrac{\partial\breve{w}}{\partial\theta}\end{bmatrix}^{\psi} \tag{10}$$

2.4 Compatibility equations

Based on the compatibility conditions and perfect bonding have:

$$\begin{aligned}
&\breve{u}^c(z_c=-0.5h_c)=\breve{u}^b(z_b=0.5h_b),\\
&\breve{v}^c(z_c=-0.5h_c)=\breve{v}^b(z_b=0.5h_b),\\
&\breve{w}^c(z_c=-0.5h_c)=\breve{w}^b(z_p=0.5h_b),\\
&\breve{u}^c(z_c=0.5h_c)=\breve{u}^t(z_t=-0.5h_t),\\
&\breve{v}^c(z_c=0.5h_c)=\breve{v}^t(z_t=-0.5h_t),\\
&\breve{w}^c(z_c=0.5h_c)=\breve{w}^t(z_t=-0.5h_t).
\end{aligned} \tag{11}$$

2.5 Extended Hamilton's principle

According to the Hamilton's principle, the relation between the motion equations and boundary edges can be obtained as below (Alipour *et al.* 2019, Ebrahimi *et al.* 2019, Esmailpoor Hajilak *et al.* 2019, Ghazanfari *et al*. 2019, Habibi *et al.* 2019a, b, Hashemi *et al*. 2019, Mohammadi *et al*. 2019, Pourjabari *et al*. 2019, Safarpour *et al.* 2019, Dai *et al*. 2021):

$$\int_{t_1}^{t_2}\left(\delta\breve{T}-\delta\breve{U}+\delta\breve{W}\right)^{\eta}dt=0 \tag{12}$$

The corresponding kinetic energy (Alipour *et al*. 2019, Ebrahimi *et al*. 2019, Esmailpoor Hajilak *et al*. 2019, Ghazanfari *et al.* 2019, Habibi *et al*. 2019a, b, Hashemi *et al.* 2019, Mohammadi *et al.* 2019, Pourjabari *et al.* 2019, Safarpour *et al*. 2019) of the rotating system would be formulated as:

$$\breve{T}^{\eta}=0.5\int_V\frac{1}{2}\rho^{\eta}\left[\left(\frac{\partial\breve{u}}{\partial t}\right)^2+\left(\frac{\partial\breve{v}}{\partial t}\right)^2+\left(\frac{\partial\breve{w}}{\partial t}\right)^2\right]^{\eta}dV \tag{13a}$$

$$\begin{aligned}
&\delta\breve{T}^{\eta}=\int_V\breve{\rho}^{\eta}\left(\frac{\partial\breve{u}}{\partial t}\frac{\partial\delta\breve{u}}{\partial t}+\frac{\partial\breve{v}}{\partial t}\frac{\partial\delta\breve{v}}{\partial t}+\frac{\partial\breve{w}}{\partial t}\frac{\partial\delta\breve{w}}{\partial t}\right)^{\eta}dV:\\
&\delta\breve{T}^{\eta}=\int_{R_1}^{R_2}\int_0^{\theta}\left[\begin{array}{l}
\left\{-\breve{I}_O\frac{\partial^2\breve{u}_0}{\partial t^2}-\breve{I}_1\frac{\partial^2\breve{u}_1}{\partial t^2}\right\}\delta\breve{u}_0+\left\{-\breve{I}_1\frac{\partial^2\breve{u}_0}{\partial t^2}-\breve{I}_2\frac{\partial^2\breve{u}_1}{\partial t^{2u_1}}\right\}\delta\breve{u}_1\\
+\left\{-\breve{I}_O\frac{\partial^2\breve{v}_0}{\partial t^2}-\breve{I}_1\frac{\partial^2\breve{v}_1}{\partial t^2}\right\}\delta\breve{v}_0+\left\{-\breve{I}_1\frac{\partial^2\breve{v}_0}{\partial t^2}-\breve{I}_2\frac{\partial^2\breve{v}_1}{\partial t^2}\right\}\delta\breve{v}_1\\
+\left\{-\breve{I}_O\frac{\partial^2\breve{w}_0}{\partial t^2}\right\}\delta\breve{w}_0
\end{array}\right]^{\eta}RdRd\theta
\end{aligned} \tag{13b}$$

where (Zhang *et al*. 2020, Wang *et al*. 2021):

$$\left\{\breve{I}_i\right\}=\int_{-\frac{h}{2}}^{\frac{h}{2}}\breve{\rho}^{\eta}(z)\left\{z^i\right\}dZ,i=0:6 \tag{14}$$

Also, the strain energy of the current composite structure would be obtained as:

$$\begin{aligned}
\delta\breve{U}^{\eta}&=\iiint_V\breve{\sigma}_{ij}^{\eta}\delta\breve{\varepsilon}_{ij}^{\eta}dV\\
&=\int_A\left[\begin{array}{l}
\left(\breve{N}_{RR}\frac{\partial\delta\breve{u}_0}{\partial R}+\breve{M}_{RR}\frac{\partial\delta\breve{u}_1}{\partial R}\right)+\left(\begin{array}{l}\breve{N}_{\theta\theta}\frac{\partial\delta\breve{v}_0}{R\partial\theta}+\breve{M}_{\theta\theta}\frac{\partial\delta\breve{v}_1}{R\partial\theta}\\+\breve{N}_{\theta\theta}\frac{\delta\breve{u}_0}{R}+\breve{M}_{\theta\theta}\frac{\delta\breve{u}_1}{R}\end{array}\right)\\
+\left(\begin{array}{l}\breve{N}_{R\theta}\frac{\partial\delta\breve{v}_0}{\partial R}+\breve{M}_{R\theta}\frac{\partial\delta\breve{v}_1}{\partial R}+\\\breve{N}_{R\theta}\frac{\partial\delta\breve{u}_0}{R\partial\theta}+\breve{M}_{R\theta}\frac{\partial\delta\breve{u}_1}{R\partial\theta}\\-\breve{N}_{R\theta}\frac{\delta\breve{v}_0}{R}-\breve{M}_{R\theta}\frac{\delta\breve{v}_1}{R}\end{array}\right)+\left(\breve{N}_{Rz}\left(\delta\breve{u}_1+\frac{\partial\delta\breve{w}_0}{\partial R}\right)\right)\\
+\left(\breve{N}_{\theta z}\left(\delta\breve{v}_1+\frac{\partial\delta\breve{w}_0}{R\partial\theta}\right)\right)
\end{array}\right]^{\eta}dA
\end{aligned} \tag{15}$$

which (Shahgholian-Ghahfarokhi *et al*. 2019, Chen *et al*. 2020, Rahimi *et al*. 2020, Chi *et al*. 2021, Safarpour *et al*. 2021):

$$\begin{aligned}
&\left\{\breve{N}_{RR},\breve{M}_{RR}\right\}^{\eta}=\int_z\left\{\breve{\sigma}_{RR},z\breve{\sigma}_{RR}\right\}^{\eta}dz;\\
&\left\{\breve{N}_{\theta\theta},\breve{M}_{\theta\theta}\right\}^{\eta}=\int_z\left\{\breve{\sigma}_{\theta\theta},z\breve{\sigma}_{\theta\theta}\right\}^{\eta}dz;\\
&\left\{\breve{N}_{Rz},\breve{M}_{Rz}\right\}^{\eta}=\int_z\left\{\breve{\sigma}_{Rz},z\breve{\sigma}_{Rz}\right\}^{\eta}dz;.\\
&\left\{\breve{N}_{R\theta},\breve{M}_{R\theta}\right\}^{\eta}=\int_z\left\{\breve{\sigma}_{R\theta},z\breve{\sigma}_{R\theta}\right\}^{\eta}dz;\\
&\left\{\breve{N}_{\theta z},\breve{M}_{\theta z}\right\}^{\eta}=\int_z\left\{\breve{\sigma}_{\theta z},z\breve{\sigma}_{\theta z}\right\}^{\eta}dz.
\end{aligned} \tag{16}$$

Afterward, the variation of the work induced by thermal gradient is formulated as

$$\delta\breve{W}^{\eta}=\int\left[\breve{N}^T\frac{\partial^2\breve{w}}{\partial R^2}+\frac{N^T}{R}\frac{\partial\breve{w}}{\partial R}+\frac{N^T}{R^2}\frac{\partial^2\breve{w}}{\partial\theta^2}\right]^{\eta}dA \tag{17}$$

Force resultant of thermal loading $\breve{N}^T$ involved in Eq. (17) can be determined by following relation

$$\breve{N}^T=\int_{-h/2}^{h/2}(\breve{Q}_{11}+\breve{Q}_{12})\breve{\alpha}_C(\breve{T}-\breve{T}_0)dz \tag{18}$$

Eventually, governing equations and corresponding boundary conditions can be derived by substituting Eqs. (13b), (15), and (17) in Hamilton's principle (Eq. (12)) that can be given by the following Eqs.:

$\delta\breve{u}_0^{\eta}$:

$$\frac{\partial}{\partial R}\breve{N}_{RR}{}^{\eta}-\frac{\breve{N}_{\theta\theta}{}^{\eta}-\breve{N}_{RR}{}^{\eta}}{R}+\frac{\partial}{R\partial\theta}\breve{N}_{R\theta}{}^{\eta}=\breve{I}_0{}^{\eta}\frac{\partial^2\breve{u}_0{}^{\eta}}{\partial t^2}+\breve{I}_1{}^{\eta}\frac{\partial^2\breve{u}_1{}^{\eta}}{\partial t^2} \tag{19a}$$

$\delta\breve{v}_0^{\eta}$:

$$\frac{\partial}{R\partial\theta}\breve{N}_{\theta\theta}{}^{\eta}+\frac{2\breve{N}_{R\theta}{}^{\eta}}{R}+\frac{\partial}{\partial R}\breve{N}_{R\theta}{}^{\eta}=\breve{I}_0{}^{\eta}\frac{\partial^2\breve{v}_0{}^{\eta}}{\partial t^2}+\breve{I}_1{}^{\eta}\frac{\partial^2\breve{v}_1{}^{\eta}}{\partial t^2} \tag{19b}$$

$$\delta\breve{w}_0^{\eta}:$$
$$\frac{\partial}{\partial R}\left(\breve{N}_{Rz}{}^{\eta}\right)+\frac{\partial}{R\partial\theta}\left(\breve{N}_{\theta z}{}^{\eta}\right)+\frac{\partial}{\partial R}\breve{N}_{Rz}{}^{\eta}+\frac{\partial}{R\partial\theta}\breve{N}_{\theta z}{}^{\eta}$$
$$-\breve{N}^{T}\frac{\partial^2\breve{w}}{\partial R^2}-\frac{N^T}{R}\frac{\partial\breve{w}}{\partial R}-\frac{N^T}{R^2}\frac{\partial^2\breve{w}}{\partial\theta^2}=\left(\breve{I}_0{}^{\eta}\frac{\partial^2\breve{w}_0{}^{\eta}}{\partial t^2}\right) \quad (19c)$$

$$\delta u_1^{\eta}:$$
$$\frac{\partial}{\partial R}\breve{M}_{RR}{}^{\eta}-\frac{\breve{M}_{\theta\theta}{}^{\eta}-\breve{M}_{RR}{}^{\eta}}{R}+\frac{\partial}{R\partial\theta}\breve{M}_{R\theta}{}^{\eta}-\breve{N}_{Rz}{}^{\eta}=\breve{I}_1{}^{\eta}\frac{\partial^2\breve{u}_0{}^{\eta}}{\partial t^2}+\breve{I}_2{}^{\eta}\frac{\partial^2\breve{u}_1{}^{\eta}}{\partial t^2} \quad (19d)$$

$$\delta\breve{v}_1:$$
$$\frac{\partial}{R\partial\theta}\breve{M}_{\theta\theta}+\frac{2}{R}\breve{M}_{R\theta}+\frac{\partial}{\partial R}\breve{M}_{R\theta}-\breve{M}_{\theta z}=\breve{I}_1{}^{\eta}\frac{\partial^2\breve{v}_0}{\partial t^2}+\breve{I}_2{}^{\eta}\frac{\partial^2\breve{v}_1}{\partial t^2} \quad (19e)$$

Also, general associated boundary conditions can be given by:

$$\begin{aligned}
&\delta\breve{u}_0{}^{\eta}=0 \quad or \quad \breve{N}_{RR}{}^{\eta}\breve{n}_R+\frac{1}{R}\breve{N}_{R\theta}{}^{\eta}\breve{n}_\theta=0\\
&\delta\breve{v}_0{}^{\eta}=0 \quad or \quad \breve{N}_{R\theta}{}^{\eta}\breve{n}_R+\frac{1}{R}\breve{N}_{\theta\theta}{}^{\eta}\breve{n}_\theta=0\\
&\delta\breve{w}_0{}^{\eta}=0 \quad or \quad \breve{N}_{Rz}{}^{\eta}\breve{n}_R+\left(\frac{N_{\theta z}}{R}\right)^{\eta}\breve{n}_\theta=0\\
&\delta\breve{u}_1{}^{\eta}=0 \quad or \quad \breve{M}_{RR}{}^{\eta}\breve{n}_R+\left(\frac{\breve{M}_{R\theta}}{R}\right)^{\eta}\breve{n}_\theta=0\\
&\delta\breve{v}_1{}^{\eta}=0 \quad or \quad \breve{M}_{R\theta}{}^{\eta}\breve{n}_R+\left(\frac{\breve{M}_{\theta\theta}}{R}\right)^{\eta}\breve{n}_\theta=0
\end{aligned} \quad (20)$$

It should be noted that, based on Eq. (11) the numbers of unknown variables are declined from 15 to 9. So, the total number of unknowns in the face sheet and core are reduced to 9.

3. Solution procedure

In this part of the present work, we displayed a solution procedure which is called GDQM for solving the formulation of the current problem. GDQM can be used as a strong solver in many systems and structures such as (Zhang *et al*. 2020, Liu *et al*. 2021). The first assumption in this is as follows:

$$\frac{\partial^n g}{\partial r^n}=\sum_{m=1}^{M}D^{(n)}{}_{j,m}g_{m,k} \quad (21)$$

here, $D^{(n)}$ shows weighting factors for the n^{th}-order derivative in the orientation of its radius, that can be extracted as follows (Cheshmeh *et al*., Ghabussi *et al*. 2020, Jermsittiparsert *et al*. 2020, Moayedi *et al*. 2020, Najaafi *et al*. 2020, Oyarhossein *et al*. 2020, Safarpour *et al*. 2020, Shariati *et al*. 2020, Zhang *et al*. 2020):

$$\begin{aligned}
&D_{ij}^{(1)}=-\sum_{j=1,i\neq j}^{n}D_{ij}^{(1)} && i=j\\
&D_{ij}^{(1)}=\frac{N\left(r_i\right)}{\left(r_i-r_j\right)M\left(r_j\right)} && i,j=1,2,...,\mathrm{n}\ \text{ and }\ \mathrm{i}\neq\mathrm{j}
\end{aligned} \quad (22)$$

where,

$$M\left(r_i\right)=\prod_{j=1,j\neq i}^{n}\left(r_i-r_j\right) \quad (23)$$

The derivatives of Eq. (21) can be written as the following equations:

$$\begin{aligned}
&D_{ii}^{(n)}=-\sum_{j=1,i\neq j}^{n}D_{ij}^{(n)}\\
&1\leq n\leq N-1 \text{ while } \ j,i=1,2,...,N\\
&D_{ij}^{(n)}=r\left[D_{ij}^{(n-1)}D_{ij}^{(1)}-\frac{D_{ij}^{(n-1)}}{\left(r_i-r_j\right)}\right]\\
&\mathrm{i}\neq\mathrm{j},2\leq n\leq N-1 \text{ while } \ j,i=1,2,...,N.
\end{aligned} \quad (24)$$

Also, using Chebyshev polynomials greed points, the seed along with r-axes can be distributed as:

$$r_i=\frac{R_0-R_i}{2}\left(1-\cos\left(\frac{(i-1)}{(N_i-1)}\pi\right)\right)+R_i \qquad i=1,2,3,\ldots,N_i \quad (25)$$

Also, displacement fields of a disk can be given by:

$$\begin{Bmatrix}\breve{u}_0\\ \breve{v}_0\\ \breve{w}_0\\ \breve{u}_1\\ \breve{v}_1\end{Bmatrix}=\sum_{n=1}^{\infty}\begin{Bmatrix}\breve{u}_{0n}(R)\times\prod\\ \breve{v}_{0n}(R)\times\coprod\\ \breve{w}_{0n}(R)\times\prod\\ \breve{u}_{1n}(R)\times\prod\\ \breve{v}_{1n}(R)\times\coprod\end{Bmatrix}e^{i\omega t} \quad (26)$$

where $\prod=\sin(n\theta)$, and $\prod=\cos(n\theta)$.

Finally, the GDQ form of the formulations with the aid of boundary condition equations can be given by:

$$\left\{\begin{bmatrix}\left[\breve{M}_{DD}\right] & \left[\breve{M}_{DB}\right]\\ \left[\breve{M}_{BD}\right] & \left[\breve{M}_{BB}\right]\end{bmatrix}\breve{\omega}_n^2+\begin{bmatrix}\left[\breve{K}_{DD}\right] & \left[\breve{K}_{DB}\right]\\ \left[\breve{K}_{BD}\right] & \left[\breve{K}_{BB}\right]\end{bmatrix}\right\}\begin{Bmatrix}\breve{\delta}_D\\ \breve{\delta}_B\end{Bmatrix}=0 \quad (27)$$

Finally, by solving the bellow equation, frequency information, and displacement fields of the structure can be extracted using GDQM.

$$\breve{K}^{*}+\breve{M}^{*}\breve{\omega}^2=0 \quad (28)$$

To reduce computational complexity, the frequency of the disk is non-dimensional as follows

$$\bar{\omega}_n=\breve{\omega}R_o^2\sqrt{\frac{\breve{\rho}_m}{\breve{E}_m}} \quad (29)$$

4. Deep learning-based comparative study

Recently, deep learning attracted many researchers to use it as the practical tool in different areas such as classification, regression and segmentation tasks (Chi *et al*. 2021). Therefore, the authors designed a deep neural network (DNN) with optimized parameters determined by

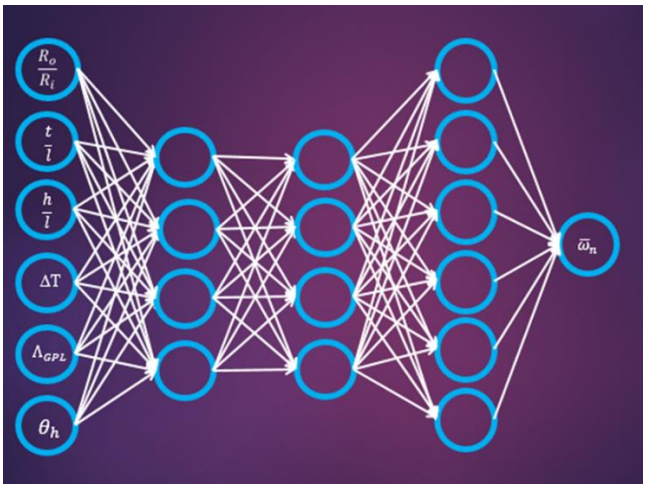

Fig. 3 Schematic of the structure of fully-connected deep neural network

ADADELTA (an abbreviation for adaptive delta). The set of $X = \left\{\frac{R_o}{R_i}, \frac{t}{l}, \frac{h}{l}, \Delta T, \Lambda_{GPL}, \theta_h\right\}^T$ is chosen as the input of regression-based DNN to predict the non-dimensional natural frequency $\hat{Y} = \bar{\omega}_n$. The schematic of the mentioned DNN is displayed in Fig. 3.

The input of the perceptron is the output of the units constituting the previous layer of the network. To obtain the output of the computational unit, the value of each input must be mathematically manipulated with weights and biases. To be more informed about the basics of the neural network approach, readers may check the contents of (White 1992) as the reference. The mean squared error (MSE) is the metric selected in this study to evaluate the accuracy of the DNN in prediction of the natural frequency. Following equation defines MSE as the mean of the squared discrepancy between the expected frequency and predicted one.

$$\mathrm{MSE}=\frac{1}{n}\sum_{i=1}^{n}\left(Y-\hat{Y}\right)^2 \tag{30}$$

4.1 ADADELTA optimization to tune the DNN parameters

ADADELTA is chosen as the optimization approach to find proper weights and biases in order to minimize the MSE. The main advantages of ADADELTA are listed as below:

- This approach sets the learning rate automatically
- ADADELTA is not sensitive to the values of the hyper parameters
- This approach has the capability to use in local environment as well as the distributed one

To update the neural network parameters (weights and biases) at each steps of iteration (epoch), one can use the following relation

$$h_{t+1} = h_t + Vh_t \tag{31}$$

$$V\chi_t = -\eta \frac{\partial f(\chi_t)}{\partial \chi_t}$$

here, η indicates the initial learning rate. In order to simplify denoting the gradient of the involved parameters at the t[th] epoch, we use G_t in place of $\frac{\partial f(h_t)}{\partial h_t}$.

To obtain the update of the biases and weights, it is required to calculate the root mean square of the gradient at the current epoch by following relation

$$\mathrm{RMS}\left[\Re_t\right] = \sqrt{E\left[\Re_t^2\right] + \varepsilon} \tag{32}$$

here, ε is a constant. It should be said that $E\left[\Re_t^2\right]$ denotes the expected value of the squared gradient which can be determined according to the subsequent expression

$$E\left[\Re_t^2\right] = \rho E\left[\Re_{t-1}^2\right] + (1-\rho)\Re_t^2 \tag{33}$$

here, ρ represents the decay rate. Utilizing Eq. (32) and Eq. (33), one can acquire the update of the mentioned parameters as below

$$Vh_t = -\frac{\eta}{RMS\left[\Re_t\right]}\Re_t \tag{34}$$

To summarize the required steps to find the optimum values of the parameters, following pseudo-code is provided as Table. 1.

As illustrated in this figure, ADADELTA outperforms the other optimizers and reaches the ultimate value of the error during the lowest number. Accordingly, ADADELTA can be sorted as one of the high-speed optimizers with the capability to reach the lower value of the minimum error among the famous optimization approaches.

As already discussed, ADADELTA optimizer was used to tune the parameters of DNN to make a regression-based predictor of vibration response of disk. The activation function of the hidden layers acts according to Rectified linear unit (ReLU). The process of training is done by using the 70% of the dataset. The accuracy of the results is

Table 1 The steps needed to apply ADADELTA to optimize the parameters of DNN

Computing ADADELTA update at time t	
Require	Consider the values of ρ and ε parameters, guess $\hbar_t$
1	Initialize accumulation variables $E\,[\Re^2]_0 = 0, E\,[\Delta\hbar^2]_0 = 0$
2	for t= 1 :T do %% Loop over # of updates
3	Compute Gradient: $\Re_L$
4	Accumulate Gradient: $E\,[\Re^2]_t = \rho E\,[\Re^2]_{t-1} + (1-\rho)\Re_t^2$
5	Compute Update: $\Delta x_t = -\frac{RMS[\Delta\hbar]_{t-1}}{RMS[\Re]_t}\Re_t$
6	Accumulate Updates: $E[\Delta\hbar^2]_t = \rho E[\Delta\hbar^2]_{t-1} + (1-\rho)\Delta\hbar_t^2$
7	Apply Update: $\hbar_{t+1} = \hbar_t + \Delta\hbar_t$
8	end for loop

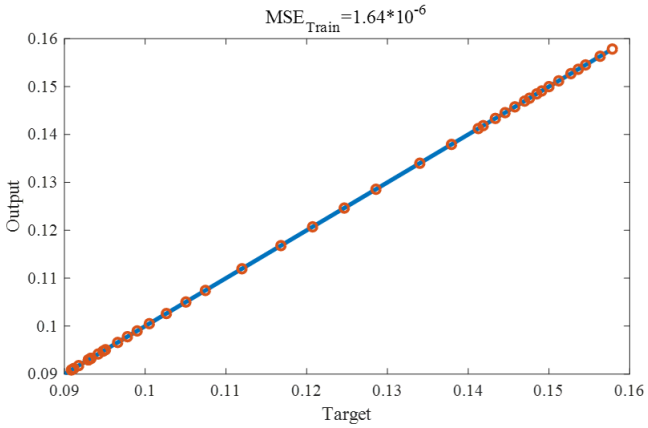

Fig. 4 Prediction performance of DNN model toward training data

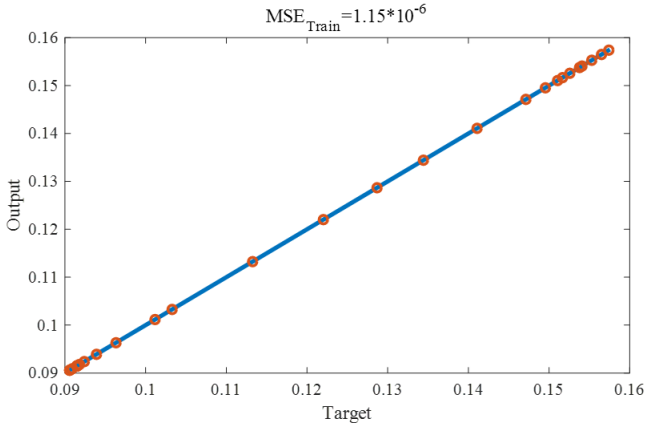

Fig. 5 Prediction performance of DNN model toward test data

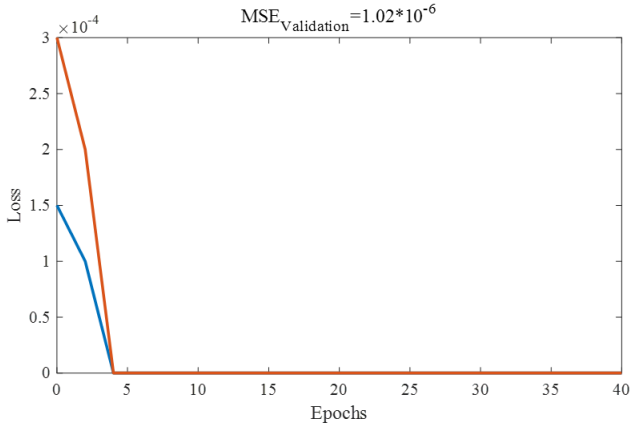

Fig. 6 The variation of MSE of training and validation datapoints against the number of iterations

Table 2 Material properties of the GPLRC structure (Shahverdi *et al*. 2019)

Graphene Platelets	$\breve{E}^{GPL}$	$\breve{\nu}^{GPL}$	$\breve{\rho}^{GPL}$	l^{GPL}	t^{GPL}	w^{GPL}
	[Gpa]		$[kg/m^3]$	[μm]	[nm]	[μm]
	1010	0.186	1062.5	2.5	1.5	1.5
Epoxy (resin)	$\breve{E}^{m}$	$\breve{\nu}^{m}$	$\breve{\rho}^{m}$			
	[Gpa]		$[kg/m^3]$			
	2.85	0.34	1200			

examined by analyzing the MSE of the testing and validation section of dataset. The outcomes of training process are shown in Fig. 4. Based on this figure, the discrepancy between the expected frequencies and the predicted ones are completely desirable. Because, the predicted points have very low distance from the fitting line. The small MSE of training process ($MSE_{Train} = 1.64 * 10^{-6}$) indicates the superb capabilities of ADADELTA to find the appropriate parameters to tune the DNN. To rely on the astonishing performance of the mentioned fully-connected DNN, it is required to investigate the accuracy of the approach toward validation and test sets.

Fig. 5 explores the accuracy of predictions carried out by DNN for the test dataset. Based on this figure, the discrepancy between the expected frequencies and the predicted ones are completely desirable. Because, the predicted points have very low distance from the fitting line. The small MSE of test process ($MSE_{Test} = 1.15 * 10^{-6}$) indicates the power of the mentioned approach to predict the vibration of the system.

The variation of MSE of training and validation datapoints against the number of iterations is displayed in Fig. 6. As demonstrated, both validation and training losses significantly decline by growth of the epochs number. It should be noted that $MSE_{Validation} = 1.02 * 10^{-6}$ during 40 epochs.

5. Material and validation

Since the final intention of this studies will be enhancements within side the dynamics of a disk, a well-known reinforcement referred to as graphene nanoplatelets bolstered composites are applied, whilst mechanical houses of those reinforcements together with the resin epoxy used on this studies are disclosed in Table 2.

For accuracy of the current study, numerical outcomes are as compared with the ones of Ref. (Han *et al*. 1999) in Table 3 for an isotropic round plate. Accordingly, an outstanding settlement is suggested from the desk which means that the most discrepancy among the outcomes is about 1%. As properly as this, it is able to be visible that with the aid of using growing the mode number, the herbal frequency has a tendency to increase. However, those adjustments are reversed with the aid of using growing the h/Ro. It way with the aid of using growing the h/Ro, the herbal frequency decreases.

6. Numerical results

The offered facts in Fig. 7 encounters us with an research at the frequency conduct of the sandwich disk with honeycomb center and FG-GPLRC face sheet with the aid of using thinking about the FG styles and outer to internal radius ratio (R_o/R_i) effects. For every R_o/R_i and boundary conditions, the very best and lowest frequency are for the structure, that's made with the aid of using FG-X and FG-O, respectively.

Table 3 Comparison of obtained dynamic response for different *h/Ro* with the result of Ref (Han *et al*. 1999)

h/Ro	Mode number = 1 (Ref (Han *et al*. 1999))	Mode number = 1 (Present)	Mode number = 2 (Ref (Han *et al*. 1999))	Mode number = 2 (Present)	Mode number = 3 (Ref (Han *et al*. 1999))	Mode number = 3 (Present)	Mode number = 4 (Ref (Han *et al*. 1999))	Mode number = 4 (Present)
0.001	59.819	62.421081	198.04	202.74802	415.12	417.733480	711.12	715.369157
0.05	57.250	59.724417	177.84	180.65834	344.35	346.333165	541.41	536.508525
0.1	51.219	53.472342	142.71	144.05551	252.22	257.196138	369.86	368.652369
0.15	44.443	45.565987	114.18	116.17581	192.05	190.569853	272.49	271.256987

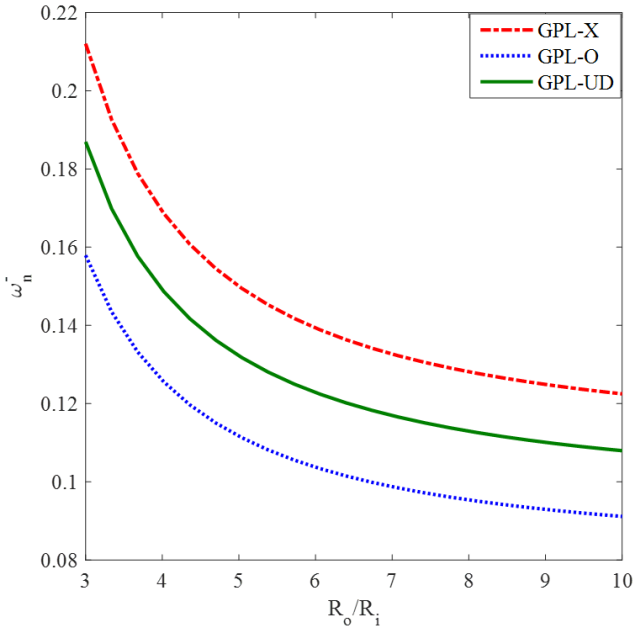

Fig. 7 Frequency performance of the multi-layer structure with lattice core and compositionally layers for various FG patterns and R_o/R_i parameters

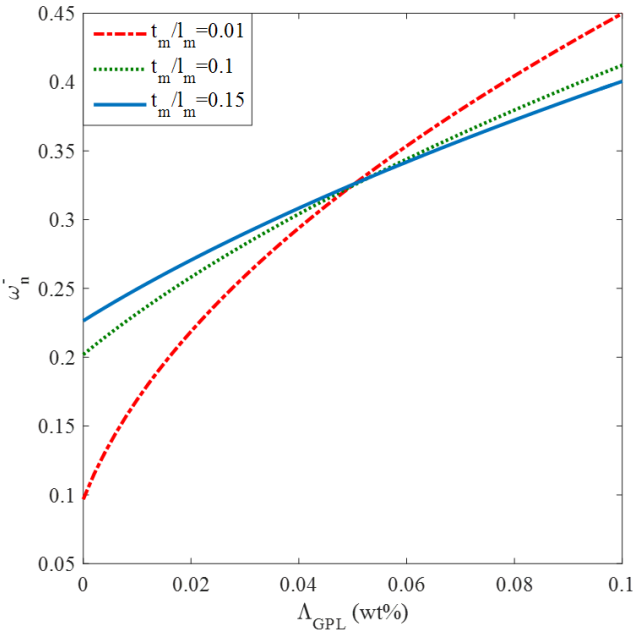

Fig. 9 Frequency performance of the multi-layer structure with lattice core and compositionally layers for various t_m/l_m and Λ_{GPL} parameters

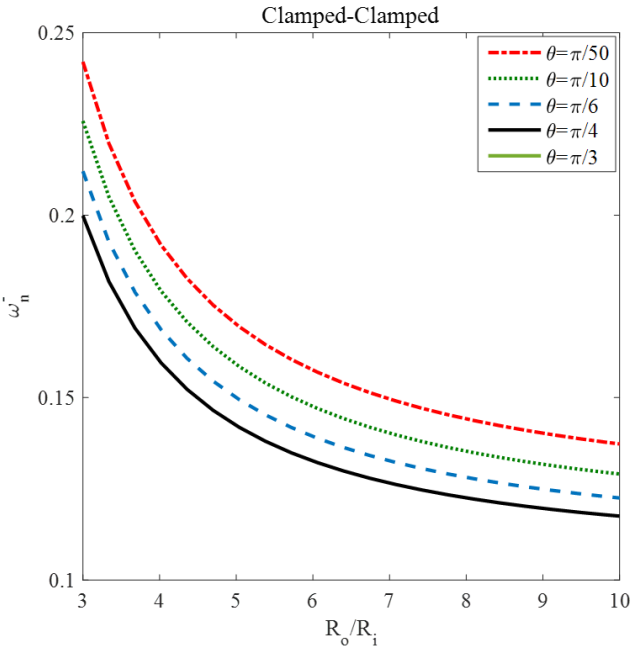

Fig. 8 frequency performance of the multi-layer structure with lattice core and compositionally layers for various θ and R_o/R_i parameters

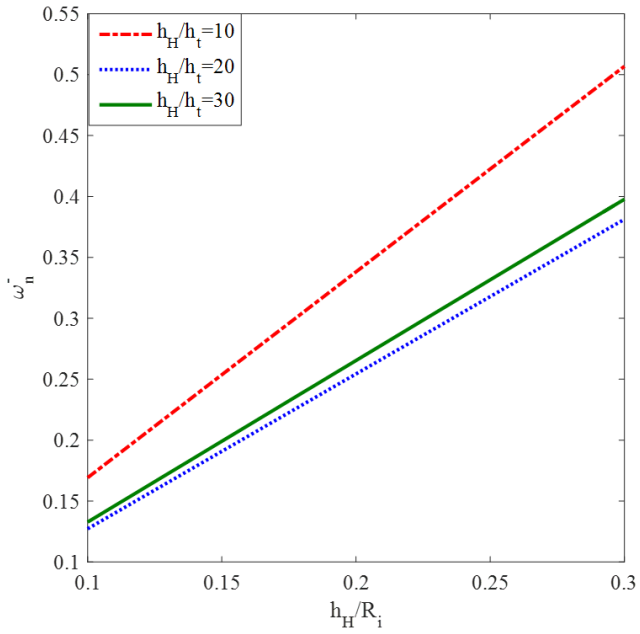

Fig. 10 Frequency information of the multi-layer structure with lattice core and compositionally layers for various h_H/R_i and h_H/h_t parameters

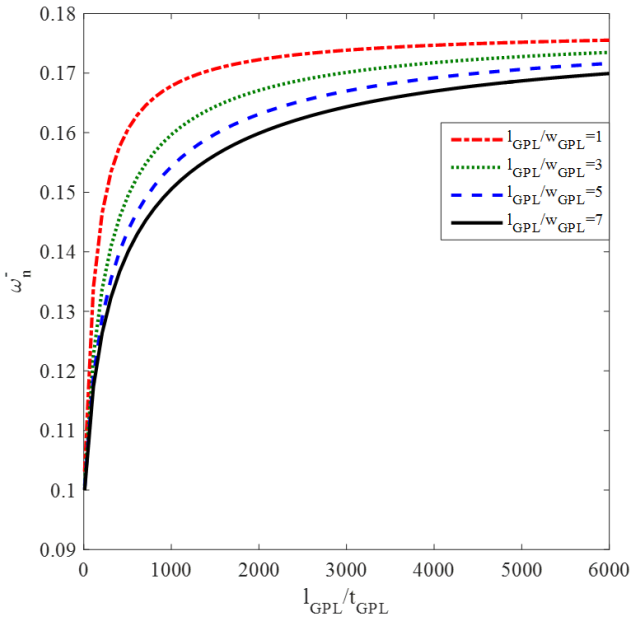

Fig. 11 Frequency information of the multi-layer structure with lattice core and compositionally layers for various l_{GPL}/t_{GPL} and l_{GPL}/w_{GPL} parametrs

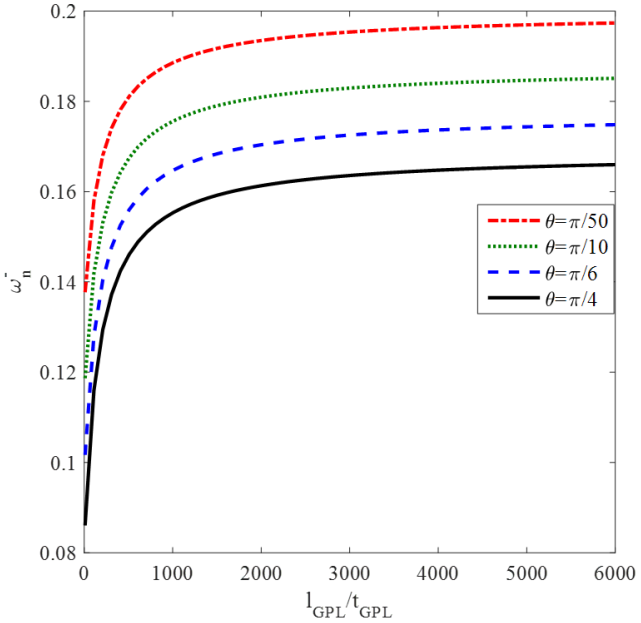

Fig. 12 Frequency information of the multi-layer structure with lattice core and compositionally layers for various l_{GPL}/t_{GPL} and θ parametrs

Dates in Fig. 9 offer a look at the frequency conduct of the multi-layer structure with honeycomb center and compositionally layers via way of means of having attentions to the thickness to period ratio of the weight fraction of GPLs (Λ_{GPL}), and GPLs (t_m/l_m) effects. For every boundary condition, and preliminary Λ_{GPL}, the very best frequency is for the structure, that's bolstered with the thicker GPLs. Also, for grater Λ_{GPL}, there's a decline withinside the frequency of the annular system because of developing up the t_m/l_m. In addition, if the t_m/l_m decreases, the dynamic reaction improves and this depend is actual for

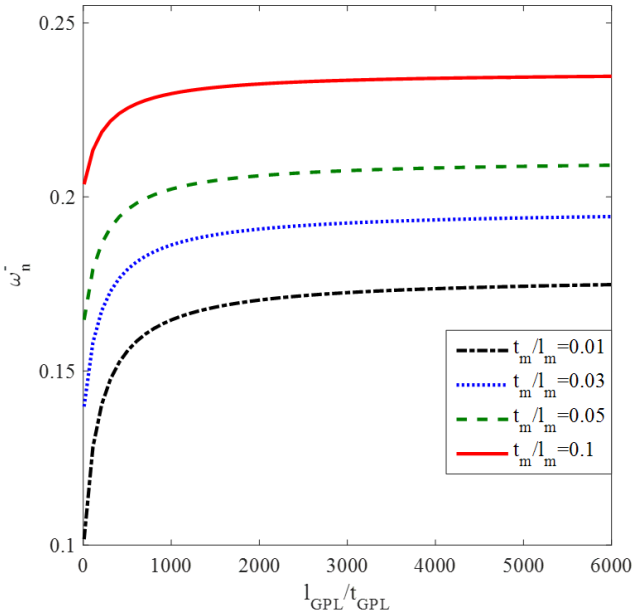

Fig. 13 Frequency information of the multi-layer annular system with lattice core and compositionally layers for different l_{GPL}/t_{GPL} and t_m/l_m parametrs

preliminary Λ_{GPL}. Also, we will see that developing the Λ_{GPL} is a cause for enhancing the frequency. Finally, primarily based totally at the Fig. 9, the relation among $\Lambda_{GPL}$and frequency conduct of the sandwich annular system with lattice center and compositionally layers has a good sized dependence on t_m/l_m.

Diagrams in Fig. 11 display a presentation on the frequency behavior of the sandwich disk with honeycomb core and GPLRC face sheet by having attentions on the ratio of length to thickness (l_{GPL}/t_{GPL}) and length to width (l_{GPL}/w_{GPL}) of GPLs and three kinds of boundary conditions. For each boundary edge and l_{GPL}/w_{GPL}, the results of Fig. 11 show that the longer the length of GPLs, the greater the stability of the system and this phenomenon is noticeable at low value of l_{GPL}/t_{GPL} and l_{GPL}/w_{GPL}. With an exact consideration to Fig. 11, it can be concluded that the effect of the width of GPLs is very noticeable at low values of l_{GPL}/t_{GPL} or thickness of the GPLs.

Diagrams in Fig. 12 display a presentation on the frequency behavior of the sandwich disk with honeycomb core and GPLRC face sheet by having attentions on the ratio of length to thickness of GPLs (l_{GPL}/t_{GPL}) and angle of the honeycomb (θ) and three kinds of boundary conditions. For each boundary edge and θ, the date of Fig. 12 proves that the longer the length of GPLs, the better the stability of the system and this phenomenon is noticeable at lower l_{GPL}/t_{GPL} and higher θ. With an exact consideration to Fig. 12, it can be concluded that the effect of the θ is very noticeable at low values of l_{GPL}/t_{GPL} or thickness of the GPLs.

Diagrams in Fig. 13 display a presentation on the frequency behavior of the multi-layer annular plate with latticd core and compositionally layers by having attentions on l_{GPL}/t_{GPL} and t_m/l_m and different boundary edges. With an exact consideration to Fig. 13, can be concluded that the

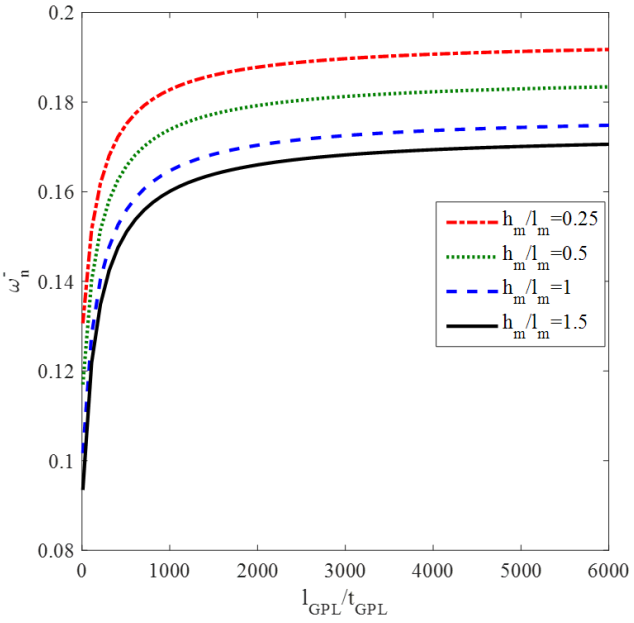

Fig. 14 Frequency information of the multi-layer annular disk with lattice core and compositionally layers for various l_{GPL}/t_{GPL} and h_m/l_m parameters

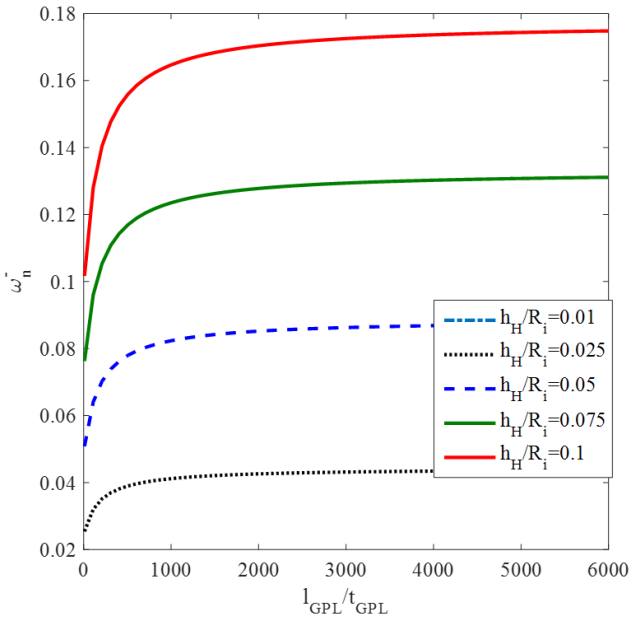

Fig. 15 Frequency information of the multi-layer system with lattice core and compositionally layers for various l_{GPL}/t_{GPL} and h_H/R_i parameters

effect of the t_m/l_m is very noticeable when the thinner GPLs are used. In other words, the higher the t_m/l_m , the higher the frequency is observed at the initial value of l_{GPL}/t_{GPL}.

Fig. 14 provides a study on the frequency behavior of the multi-layer annular system with lattice core and compositionally layers by having attentions to h_m/l_m and l_{GPL}/t_{GPL} effects. As well as boosting the dynamic response due to declining the h_m/l_m, the frequency of the multi-layer composite structure could be improved with using the thinner GPLs.

Fig. 15 studies on the dynamic behavior of the multi-

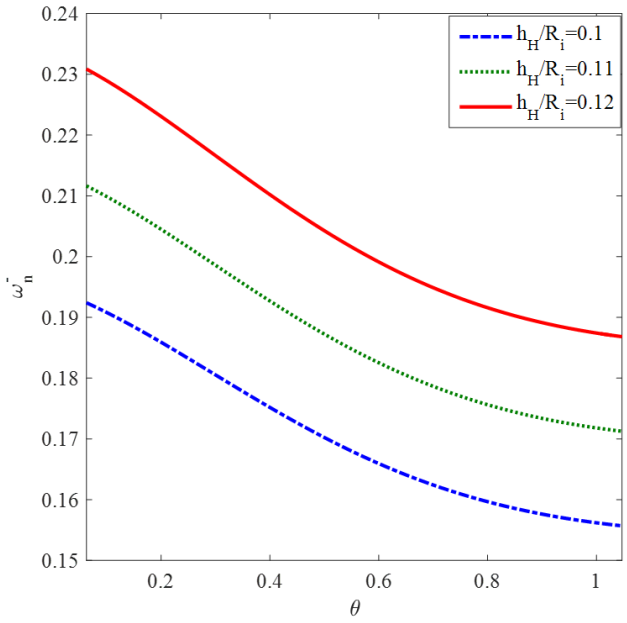

Fig. 16 Frequency information of the multi-layer system with lattice core and compositionally layers for various θ and h_H/R_i parameters

layer composite annular plate with lattice core and compositionally layers by having attentions to h_H/R_i and l_{GPL}/t_{GPL} effects. As well as improving the dynamic response due to decreasing the h_H/R_i, the frequency of the sandwich annular system could be improved with using the thinner GPLs.

The given plots in Fig. 16 offer a look at the frequency conduct of the multi-layer annular system with lattice center with recognize to the h_H/R_i and θ impacts. For every honeycomb center attitude and boundary edges, the best frequency is for the multi-layer annular system with lattice center, that's bolstered with the thicker honeycomb center. For greater explanation, for $\theta \leq 0.75$, proudly owning to boom in the θ, the frequency decreases but, for $\theta > 0.75$, there may be a development in dynamic balance of the disk because of boom in the θ.

7. Conclusions

In this article with the aid of adaptively tuned deep neural network (DNN), dynamic stability analysis of the sandwich structure was investigated. Due to finding the design-points features, the numerical solution procedure called two-dimensional generalized differential quadrature technique was applied to the ordinary differential equations of the current structure system acquired on the foundation of the kinematic theory with refined higher order terms. Also, the involved parameters with the optimum values in the fully-connected neural network mechanism were obtained via momentum-based optimizer. For modeling a moderately thick structure, higher order terms of shear deformation were chosen. For stability analysis of the current structure the design points considering the method of adaptive learning was presented. For analysis of the

current structure ‘accuracy (used for determining the design-points) was presented through than the published outcomes in the literature. The outcomes of accuracy section of the current research showed that the DNN-based model in analysis of the sandwich structure had less error than other models. The outcomes of the current report showed that radius curvature, composite patterns, angle of hexagonal middle, the thickness of compositionally layers, and geometry of the lattice core have an essential function within side the frequency traits of a sandwich annular system with lattice middle and compositionally layers.

References

Abd El Aziz, M., Hemdan, A.M., Ewees, A.A., Elhoseny, M., Shehab, A., Hassanien, A.E. and Xiong, S. (2017), “Prediction of biochar yield using adaptive neuro-fuzzy inference system with particle swarm optimization”, *Proceedings of the 2017 IEEE PES PowerAfrica*, Accra, Ghana, June.

Abdel Basset, M., El Hoseny, M., Gamal, A. and Smarandache, F. (2019a), “A novel model for evaluation Hospital medical care systems based on plithogenic sets”, *Artif. Intell. Med.*, **100**, 101710. http://doi.org/10.1016/j.artmed.2019.101710.

Abdel Basset, M., Mohamed, M., Elhoseny, M., Chiclana, F. and Zaied, A.E.-N.H. (2019b), “Cosine similarity measures of bipolar neutrosophic set for diagnosis of bipolar disorder diseases”, *Artif. Intell. Med.*, **101**, 101735. http://doi.org/10.1016/j.artmed.2019.101735.

Abdel Basset, M., Mohamed, R., Elhoseny, M., Chakrabortty, R.K. and Ryan, M. (2020), “A hybrid COVID-19 detection model using an improved marine predators algorithm and a ranking-based diversity reduction strategy”, *IEEE Access*, **8**, 79521-79540. http://doi.org/10.1109/ACCESS.2020.2990893.

Al Furjan, M., Habibi, M., Ghabussi, A., Safarpour, H., Safarpour, M. and Tounsi, A. (2020), “Non-polynomial framework for stress and strain response of the FG-GPLRC disk using three-dimensional refined higher-order theory”, *Eng. Struct.*, **228**, 111496. http://doi.org/10.1016/j.engstruct.2020.111496.

Ali, M., Jung, L.T., Abdel Aty, A.H., Abubakar, M.Y., Elhoseny, M. and Ali, I. (2020), “Semantic-k-NN algorithm: An enhanced version of traditional k-NN algorithm”, *Expert Syst. Appl.*, **151**, 113374. http://doi.org/10.1016/j.eswa.2020.113374.

Alipour, M., Torabi, M.A., Sareban, M., Lashini, H., Sadeghi, E., Fazaeli, A., Habibi, M. and Hashemi, R. (2020), “Finite element and experimental method for analyzing the effects of martensite morphologies on the formability of DP steels”, *Mech. Based Des. Struct.* **48**(5), 525-541. http://doi.org/10.1080/15397734.2019.1633343.

Amini, A., Mohammadimehr, M. and Faraji, A. (2019), “Active control to reduce the vibration amplitude of the solar honeycomb sandwich panels with CNTRC facesheets using piezoelectric patch sensor and actuator”, *Steel Compos. Struct.*, **32**(5), 671-686. http://doi.org/10.12989/scs.2019.32.5.671.

Arabnejad Khanouki, M.M., Ramli Sulong, N.H. and Shariati, M. (2011), “Behavior of through beam connections composed of CFSST columns and steel beams by finite element studying”, *Adv. Mater. Res.*, **168**, 2329-2333 http://doi.org/10.4028/www.scientific.net/AMR.168-170.2329.

Bai, B., Li, H., Zhang, W. and Cui, Y. (2020), “Application of extremum response surface method-based improved substructure component modal synthesis in mistuned turbine bladed disk”, *J. Sound Vib.*, **472**, 115210 https://doi.org/10.1016/j.jsv.2020.115210.

Cao, B., Zhao, J., Yang, P., Yang, P., Liu, X., Qi, J., Simpson, A., Elhoseny, M., Mehmood, I. and Muhammad, K. (2019), “Multiobjective feature selection for microarray data via distributed parallel algorithms “, *Future Gener. Comp. Sy.*, **100**, 952-981. http://doi.org/10.1016/j.future.2019.02.030.

Chen, H., Song, H., Li, Y. and Safarpour, M. (2020), “Hygro-thermal buckling analysis of polymer–CNT–fiber-laminated nanocomposite disk under uniform lateral pressure with the aid of GDQM”, *Eng. Comput.*, 1-25. http://doi.org/10.1007/s00366-020-01102-y.

Cheshmeh, E., Karbon, M., Eyvazian, A., Jung, D., Tran, T., Habibi, M. and Safarpour, M. “Buckling and vibration analysis of FG-CNTRC plate subjected to thermo-mechanical load based on higher-order shear deformation theory”, *Mech. Based Des. Struct.*, 1-24. http://doi.org/ 10.1080/15397734.2020.1744005.

Chi, Z., Jiang, Z., Kamruzzaman, M., Hafshejani, B.A. and Safarpour, M. (2021), “Adaptive momentum-based optimization to train deep neural network for simulating the static stability of the composite structure”, *Eng. Comput.*, 1-23 https://doi.org/10.1007/s00366-021-01335-5.

Dai, H. and Safarpour, H. (2021), “Frequency and thermal buckling information of laminated composite doubly curved open nanoshell”, *Adv. Nano Res.*, **10**(1), 1-14. http://doi.org/10.12989/anr.2021.10.1.001.

Devaraj, A.F.S., Elhoseny, M., Dhanasekaran, S., Lydia, E.L. and Shankar, K. (2020), “Hybridization of firefly and improved multi-objective particle swarm optimization algorithm for energy efficient load balancing in cloud computing environments “, *J. Parallel Distr. Com.*, **142**, 36-45. http://doi.org/10.1016/j.jpdc.2020.03.022.

Dorri, A., Kanhere, S.S. and Jurdak, R. (2019), “MOF-BC: A memory optimized and flexible blockchain for large scale networks “, *Future Gener. Comp. Sy.*, **92**, 357-373. http://doi.org/ 10.1016/j.future.2018.10.002.

Dutta, A.K., Elhoseny, M., Dahiya, V. and Shankar, K. (2020), “An efficient hierarchical clustering protocol for multihop Internet of vehicles communication”, *Transact. Emerg. Telecommun. Technol.*, **31**(5), e3690. http://doi.org/10.1002/ett.3690.

Eassa, A.M., Elhoseny, M., El-Bakry, H.M. and Salama, A.S. (2018), “NoSQL injection attack detection in web applications using RESTful service”, *Program. Comput. Soft.*, **44**(6), 435-444. http://doi.org/10.1134/S036176881901002X.

Ebrahimi, F., Hajilak, Z.E., Habibi, M. and Safarpour, H. (2019), “Buckling and vibration characteristics of a carbon nanotube-reinforced spinning cantilever cylindrical 3D shell conveying viscous fluid flow and carrying spring-mass systems under various temperature distributions”, *Proceedings of the Institution of Mechanical Engineers, Part C: Journal of Mechanical Engineering Science*, **233**(13), 4590-4605. https://doi.org/10.1177/0954406219832323.

Ebrahimi, F., Jafari, A. and Selvamani, R. (2020), “Thermal buckling analysis of magneto-electro-elastic porous FG beam in thermal environment”, *Adv. Nano Res.*, **8**(1), 83-94 https://doi.org/10.12989/anr.2020.8.1.083.

Ebrahimi, F. and Salari, E. (2019), “Effect of non-uniform temperature distributions on nonlocal vibration and buckling of inhomogeneous size-dependent beams”, *Adv. Nano Res.*, **6**(4), 377-397. https://doi.org/10.12989/anr.2018.6.4.377-397.

Elhoseny, M., Yuan, X., El Minir, H.K. and Riad, A. (2014), “Extending self-organizing network availability using genetic algorithm”, *Proceeding of the Fifth International Conference on Computing, Communications and Networking Technologies (ICCCNT)*, Hefei, China, July.

Elhoseny, M., Shehab, A. and Yuan, X. (2017), “Optimizing robot path in dynamic environments using genetic algorithm and bezier curve”, *J. Intell. Fuzzy Syst.*, **33**(4), 2305-2316. http://doi.org/10.3233/JIFS-17348.

Elhoseny, H., Elhoseny, M., Riad, A.M. and Hassanien, A.E. (2018), "A framework for big data analysis in smart cities", *International Conference on Advanced Machine Learning Technologies and Applications*, Cairo, Egypt, January.

Elhoseny, M. and Shankar, K. (2019), "Optimal bilateral filter and convolutional neural network based denoising method of medical image measurements", *Measurement*, **143**, 125-135. https://doi.org/10.1016/j.measurement.2019.04.072.

Elhoseny, M., Bian, G.B., Lakshmanaprabu, S., Shankar, K., Singh, A.K. and Wu, W. (2019a), "Effective features to classify ovarian cancer data in internet of medical things", *Comput. Netw.*, **159**, 147-156. http://doi.org/10.1016/j.comnet.2019.04.016.

Elhoseny, M., Shankar, K. and Uthayakumar, J. (2019b), "Intelligent diagnostic prediction and classification system for chronic kidney disease", *Scientific Report*, **9**(1), 1-14. http://doi.org/10.1038/s41598-019.

El-Hasnony, I.M., Barakat, S.I., Elhoseny, M. and Mostafa, R.R. (2020), "Improved feature selection model for big data analytics", *IEEE Access*. **8**, 66989-67004. http://doi.org/10.1109/ACCESS.2020.2986232.

Elsayed, W., Elhoseny, M., Sabbeh, S. and Riad, A. (2018), "Self-maintenance model for wireless sensor networks", *Comput. Electr. Eng.*, **70**, 799-812. http://doi.org/10.1016/j.compeleceng.2017.12.022.

Esmailpoor Hajilak, Z., Pourghader, J., Hashemabadi, D., Sharifi Bagh, F., Habibi, M. and Safarpour, H. (2019), "Multilayer GPLRC composite cylindrical nanoshell using modified strain gradient theory", *Mech. Based Des. Struct.*, **47**(5), 521-545. http://doi.org/10.1080/15397734.2019.1566743.

Ewees, A.A., Abd El Aziz, M. and Elhoseny, M. (2017), "Social-spider optimization algorithm for improving ANFIS to predict biochar yield ", *Proceeding of the 8th International Conference on Computing, Communication and Networking Technologies (ICCCNT)*, Delhi, India. July.

Gaber, T., Abdelwahab, S., Elhoseny, M. and Hassanien, A.E. (2018), "Trust-based secure clustering in WSN-based intelligent transportation systems", *Comput. Netw.*, **146**, 151-158. http://doi.org/ 10.1016/j.comnet.2018.09.015.

Ghabussi, A., Ashrafi, N., Shavalipour, A., Hosseinpour, A., Habibi, M., Moayedi, H., Babaei, B. and Safarpour, H. (2019), "Free vibration analysis of an electro-elastic GPLRC cylindrical shell surrounded by viscoelastic foundation using modified length-couple stress parameter", *Mech. Based Des. Struct.*, 1-25 https://doi.org/10.1080/15397734.2019.1705166.

Ghabussi, A., Habibi, M., NoormohammadiArani, O., Shavalipour, A., Moayedi, H. and Safarpour, H. (2020a), "Frequency characteristics of a viscoelastic graphene nanoplatelet–reinforced composite circular microplate", *J. Vib. Control.*, 27(1-2), 101-118. http://doi.org/ 10.1177/1077546320923930.

Ghabussi, A., Marnani, J.A. and Rohanimanesh, M.S. (2020b), "Improving seismic performance of portal frame structures with steel curved dampers", *Structures*, **24**, 27-40. http://doi.org/10.1016/j.istruc.2019.12.025.

Ghabussi, A., Asgari Marnani, J. and Rohanimanesh, M.S. (2021), "Seismic performance assessment of a novel ductile steel braced frame equipped with steel curved damper", *Structures*, **31**, 87-97, https://doi.org/10.1016/j.istruc.2021.01.073.

Ghannadpour, S. and Moradi, F. (2019), "Nonlocal nonlinear analysis of nano-graphene sheets under compression using semi-Galerkin technique", *Adv. Nano Res.*, **7**(5), 311-324. https://doi.org/10.12989/anr.2019.7.5.311.

Ghazanfari, A., Soleimani, S.S., Keshavarzzadeh, M., Habibi, M., Assempuor, A. and Hashemi, R. (2019), "Prediction of FLD for sheet metal by considering through-thickness shear stresses", *Mech. Based Des. Struct.*, 1-18. http://doi.org/10.1080/15397734.2019.1662310.

Gibson, L.J. and Ashby, M.F. (1999), *Cellular Solids: Structure and Properties*, Cambridge University Press, Cambridge, England.

Gong, C., Hu, Y., Gao, J., Wang, Y. and Yan, L. (2019), "An improved delay-suppressed sliding-mode observer for sensorless vector-controlled PMSM", *IEEE T. Ind. Electron.*, **67**(7), 5913-5923. http://doi.org/10.1109/TIE.2019.2952824.

Gunasekaran, V., Pitchaimani, J. and Chinnapandi, L.B.M. (2020), "Analytical investigation on free vibration frequencies of polymer nano composite plate: Effect of graphene grading and non-uniform edge loading", *Mater. Today Commun.*, **24**, 100910. https://doi.org/10.1016/j.mtcomm.2020.100910.

Habibi, M., Hashemabadi, D. and Safarpour, H. (2019a), "Vibration analysis of a high-speed rotating GPLRC nanostructure coupled with a piezoelectric actuator", *Eur. Phys. J. Plus.*, **134**(6), 307. https://doi.org/10.1140/epjp/i2019-12742-7.

Habibi, M., Mohammadgholiha, M. and Safarpour, H. (2019b), "Wave propagation characteristics of the electrically GNP-reinforced nanocomposite cylindrical shell", *J. Brazil. Soc. Mech. Sci. Eng.*, **41**(5), 221. http://doi.org/10.1007/s40430-019-1715-x.

Hamidian, M., Shariati, M., Arabnejad, M. and Sinaei, H. (2011), "Assessment of high strength and light weight aggregate concrete properties using ultrasonic pulse velocity technique", *Int. J. Phys. Sci.*, **6**(22), 5261-5266. http://doi.org/10.5897/IJPS11.1081.

Han, J.B. and Liew, K. (1999), "Axisymmetric free vibration of thick annular plates", *Int. J. Mech. Sci.*, **41**(9), 1089-1109. https://doi.org/10.1016/S0020-7403(98)00057-5.

Hashemi, H.R., Alizadeh, A.A., Oyarhossein, M.A., Shavalipour, A., Makkiabadi, M. and Habibi, M. (2019), "Influence of imperfection on amplitude and resonance frequency of a reinforcement compositionally graded nanostructure", *Wave. Random Complex*, 1-27. http://doi.org/10.1080/17455030.2019.1662968.

Hosseinabadi, A.A.R., Vahidi, J., Saemi, B., Sangaiah, A.K. and Elhoseny, M. (2019), "Extended genetic algorithm for solving open-shop scheduling problem", *Soft Comput.*, **23**(13), 5099-5116. http://doi.org/ 10.1007/s00500-018-3177-y.

Hu, Y., Chen, Q., Feng, S. and Zuo, C. (2020), "Microscopic fringe projection profilometry: A review", *Opt. Laser. Eng.*, 106192. https://doi.org/10.1016/j.optlaseng.2020.106192.

Huang, X., Zhang, Y., Moradi, Z. and Shafiei, N. (2021a), "Computer simulation via a couple of homotopy perturbation methods and the generalized differential quadrature method for nonlinear vibration of functionally graded non-uniform micro-tube", *Eng. Comput.*, 1-18. http://doi.org/10.1007/s00366-021-01395-7.

Huang, X., Zhu, Y., Vafaei, P., Moradi, Z. and Davoudi, M. (2021b), "An iterative simulation algorithm for large oscillation of the applicable 2D-electrical system on a complex nonlinear substrate", *Eng. Comput.*, 1-13, http://doi.org/10.1007/s00366-021-01320-y.

Hurrah, N.N., Parah, S.A., Loan, N.A., Sheikh, J.A., Elhoseny, M. and Muhammad, K. (2019), "Dual watermarking framework for privacy protection and content authentication of multimedia", *Future Gener. Comp. Sy.*, **94**, 654-673. http://doi.org/10.1016/j.future.2018.12.036.

Jalali, A., Daie, M., Nazhadan, S.V.M., Kazemi-Arbat, P. and Shariati, M. (2012), "Seismic performance of structures with pre-bent strips as a damper", *Int. J. Phys. Sci.*, **7**(26), 4061-4072. http://doi.org/10.5897/IJPS11.1324.

Javani, M., Kiani, Y. and Eslami, M. (2020), "Thermal buckling of FG graphene platelet reinforced composite annular sector plates", *Thin Wall. Struct.*, **148**, 106589. http://doi.org/10.1016/j.tws.2019.106589.

Jermsittiparsert, K., Ghabussi, A., Forooghi, A., Shavalipour, A., Habibi, M., won Jung, D. and Safa, M. (2020), "Critical voltage, thermal buckling and frequency characteristics of a thermally affected GPL reinforced composite microdisk covered with piezoelectric actuator", *Mech. Based Des. Struct.*, 1-23. http://doi.org/10.1080/15397734.2020.1748052.

Jiang, D., Wang, F., Lv, Z., Mumtaz, S., Al-Rubaye, S., Tsourdos, A. and Dobre, O. (2021), "QoE-Aware efficient content distribution scheme for satellite-terrestrial networks", *IEEE T, Mobile Comput*. http://doi.org/10.1109/TMC.2021.3074917.

Jiao, J., Ghoreishi, S.-m., Moradi, Z. and Oslub, K. (2021), "Coupled particle swarm optimization method with genetic algorithm for the static–dynamic performance of the magneto-electro-elastic nanosystem", *Eng. Comput.*, 1-15. http://doi.org/10.1007/s00366-021-01391-x.

Krishnaraj, N., Elhoseny, M., Lydia, E.L., Shankar, K. and ALDabbas, O. (2021), "An efficient radix trie-based semantic visual indexing model for large-scale image retrieval in cloud environment", *Software Prac. Exper.*, **51**(3), 489-502. http://doi.org/10.1002/spe.2834.

Krishnaraj, N., Elhoseny, M., Thenmozhi, M., Selim, M.M. and Shankar, K. (2020), "Deep learning model for real-time image compression in Internet of Underwater Things (IoUT)", *J. Real Time Image Proc.*, **17**(6), 2097-2111. http://doi.org/10.1007/s11554-019-00879-6.

Lakshmanaprabu, S., Elhoseny, M. and Shankar, K. (2019), "Optimal tuning of decentralized fractional order PID controllers for TITO process using equivalent transfer function", *Cognitive Syst. Res.*, **58** 292-303. http://doi.org/10.1016/j.cogsys.2019.07.005.

Li, B.H., Liu, Y., Zhang, A.M., Wang, W.H. and Wan, S. (2020), "A survey on blocking technology of entity resolution", *J. Comput. Sci.*, **35**(4), 769-793. http://doi.org/ 10.1007/s11390-020-0350-4.

Li, B., Liang, R., Zhou, W., Yin, H., Gao, H. and Cai, K. (2021a), "LBS meets blockchain: An efficient method with security preserving trust in SAGIN", *IEEE Internet Thing J.*, http://doi.org/10.1109/JIOT.2021.3064357.

Li, Y., Qiao, L. and Lv, Z. (2021b), "An optimized byzantine fault tolerance algorithm for consortium blockchain", *Peer-to-Peer Netw. Appl.*, 1-14. http://doi.org/10.1109/JIOT.2021.3064357.

Libo, Z., Tian, H., Chunyun, G. and Elhoseny, M. (2019), "Real-time detection of cole diseases and insect pests in wireless sensor networks", *J. Intell. Fuzzy Syst.*, **37**(3), 3513-3524. http://doi.org/ 10.3233/JIFS-179155.

Liu, D., Li, Z., Kitipornchai, S. and Yang, J. (2019), "Three-dimensional free vibration and bending analyses of functionally graded graphene nanoplatelets-reinforced nanocomposite annular plates", *Compos. Struct.*, **229**, 111453. https://doi.org/10.1016/j.compstruct.2019.111453.

Liu, M., Li, C., Cao, C., Wang, L., Li, X., Che, J., Yang, H., Zhang, X., Zhao, H. and He, G. (2021), "Walnut fruit processing equipment: Academic insights and perspectives", *Food Eng. Rev.*, 1-36. http://doi.org/10.1007/s12393-020-09273-6.

Lou, R., Lv, Z., Dang, S., Su, T. and Li, X. (2021a), "Application of machine learning in ocean data", *Multimedia Syst.*, 1-10. http://doi.org/10.1007/s00530-020-00733-x.

Lou, R., Wang, W., Li, X., Zheng, Y. and Lv, Z. (2021b), "Prediction of ocean wave height suitable for ship autopilot", *IEEE T. Intell Transp.*, http://doi.org/10.1109/TITS.2021.3067040

Lv, Z., Chen, D. and Li, J. (2021a), "Novel system design and implementation for the smart city vertical market", *IEEE Commun. Mag.*, **59**(4), 126-131. http://doi.org/10.1109/MCOM.001.2000945.

Lv, Z., Chen, D., Lou, R. and Alazab, A. (2021b), "Artificial intelligence for securing industrial-based cyber–physical systems", *Future Gener. Comput. Syst.*, **117**, 291-298. http://doi.org/ 10.1016/j.future.2020.12.001.

Lv, Z., Lou, R., Li, J., Singh, A.K. and Song, H. (2021c), "Big data analytics for 6G-enabled massive internet of things", *IEEE Internet Things J.*, **8**(7), 5350-5359. http://doi.org/10.1109/JIOT.2021.3056128.

Ma, L., Liu, X. and Moradi, Z. (2021a), "On the chaotic behavior of graphene-reinforced annular systems under harmonic excitation", *Eng. Comput.*, 1-25. http://doi.org/10.1007/s00366-020-01210-9.

Ma, R., Karimzadeh, M., Ghabussi, A., Zandi, Y., Baharom, S., Selmi, A. and Maureira-Carsalade, N. (2021b), "Assessment of composite beam performance using GWO–ELM metaheuristic algorithm", *Eng. Comput.*, 1-17. http://doi.org/10.1007/s00366-021-01363-1.

Ma, X., Zhang, K., Zhang, L., Yao, C., Yao, J., Wang, H., Jian, W. and Yan, Y. (2021c), "Data-driven niching differential evolution with adaptive parameters control for history matching and uncertainty quantification", *SPE J.*, **26**(2), 993-1010. http://doi.org/10.2118/205014-PA.

Metawa, N., Elhoseny, M., Hassan, M.K. and Hassanien, A.E. (2016), "Loan portfolio optimization using genetic algorithm: a case of credit constraints", *Proceeding of the 12th International Computer Engineering Conference (ICENCO)*, Cairo, Egypt, February.

Moayedi, H., Darabi, R., Ghabussi, A., Habibi, M. and Foong, L.K. (2020), "Weld orientation effects on the formability of tailor welded thin steel sheets", *Thin Wall. Struct.*, **149** 106669. http://doi.org/ 10.1016/j.tws.2020.106669.

Mohammadhassani, M., Akib, S., Shariati, M., Suhatril, M. and Arabnejad Khanouki, M.M. (2014), "An experimental study on the failure modes of high strength concrete beams with particular references to variation of the tensile reinforcement ratio", *Eng. Fail. Anal.*, **41**, 73-80. https://doi.org/10.1016/j.engfailanal.2013.08.014.

Mohammadi, A., Lashini, H., Habibi, M. and Safarpour, H. (2019), "Influence of viscoelastic foundation on dynamic behaviour of the double walled cylindrical inhomogeneous micro shell using MCST and with the aid of GDQM", *J. Solid Mech.*, **11**(2), 440-453. http://doi.org/10.22034/jsm.2019.665264.

Mohanty, S.N., Lydia, E.L., Elhoseny, M., Al Otaibi, M.M.G. and Shankar, K. (2020), "Deep learning with LSTM based distributed data mining model for energy efficient wireless sensor networks", *Phys. Commun.*, **40**, 101097. http://doi.org/10.1016/j.phycom.2020.101097.

Moradi, Z., Davoudi, M., Ebrahimi, F. and Ehyaei, A.F. (2021), "Intelligent wave dispersion control of an inhomogeneous micro-shell using a proportional-derivative smart controller", *Wave Random Complex*, 1-24. http://doi.org/10.1080/17455030.2021.1926572.

Morasaei, A., Ghabussi, A., Aghlmand, S., Yazdani, M., Baharom, S. and Assilzadeh, H. (2021), "Simulation of steel–concrete composite floor system behavior at elevated temperatures via multi-hybrid metaheuristic framework", *Eng. Comput.*, 1-16. http://doi.org/10.1007/s00366-020-01228-z.

Muhammad, K., Khan, S., Elhoseny, M., Ahmed, S.H. and Baik, S.W. (2019), "Efficient fire detection for uncertain surveillance environment", *IEEE T. Ind. Inform.*, **15**(5), 3113-3122. http://doi.org/10.1109/TII.2019.2897594.

Mukhopadhyay, T. and Adhikari, S. (2016), "Free-vibration analysis of sandwich panels with randomly irregular honeycomb core", *J. Eng. Mech.*, **142**(11), 06016008. http://doi.org/ 10.1061/(ASCE)EM.1943-7889.0001153.

Murugan, B., Elhoseny, M., Shankar, K. and Uthayakumar, J. (2019), "Region-based scalable smart system for anomaly detection in pedestrian walkways", *Comput. Electr. Eng.*, **75**,

146-160. http://doi.org/10.1016/j.compeleceng.2019.02.017.

Naghipour, M., Niak, K.M., Shariati, M. and Toghroli, A. (2020), "Effect of progressive shear punch of a foundation on a reinforced concrete building behavior", *Steel Compos. Struct.*, **35**(2), 279-294. https://doi.org/10.12989/scs.2020.35.2.279.

Najaafi, N., Jamali, M., Habibi, M., Sadeghi, S., Jung, D.w. and Nabipour, N. (2020), "Dynamic instability responses of the substructure living biological cells in the cytoplasm environment using stress-strain size-dependent theory", *J. Biomol. Struct. Dyn.*, 39(7), 2543-2554. http://doi.org/10.1080/07391102.2020.1751297.

Nasrollahi, S., Maleki, S., Shariati, M., Marto, A. and Khorami, M. (2018), "Investigation of pipe shear connectors using push out test", *Steel Compos. Struct.*, **27**(5), 537-543. http://doi.org/10.12989/scs.2018.27.5.537.

Olia, A.S.R., Oliaei, M. and Heidarzadeh, H. (2021), "Performance of ground anchored walls subjected to dynamic and pseudo-static loading", *Civil Eng. J.*, **7**(6). http://doi.org/10.28991/cej-2021-03091703.

Olia, A.S.R. and Perić, D. (2021), "Thermomechanical soil–structure interaction in single energy piles exhibiting reversible interface behavior", *Int. J. Geomech.*, **21**(5), 04021065. https://doi.org/10.1061/(ASCE)GM.1943-5622.0002014.

Oyarhossein, M.A., Alizadeh, A.A., Habibi, M., Makkiabadi, M., Daman, M., Safarpour, H. and Jung, D.W. (2020), "Dynamic response of the nonlocal strain-stress gradient in laminated polymer composites microtubes", *Scientific Report.*, **10**(1), 5616 10.1038/s41598-020-61855-w.

Pourjabari, A., Hajilak, Z.E., Mohammadi, A., Habibi, M. and Safarpour, H. (2019), "Effect of porosity on free and forced vibration characteristics of the GPL reinforcement composite nanostructures", *Comput. Math. Appl.*, **77**(10), 2608-2626. http://doi.org/10.1016/j.camwa.2018.12.041.

Puri, V., Jha, S., Kumar, R., Priyadarshini, I., Abdel-Basset, M., Elhoseny, M. and Long, H.V. (2019), "A hybrid artificial intelligence and internet of things model for generation of renewable resource of energy", *IEEE Access*, **7**, 111181-111191. http://doi.org/10.1109/ACCESS.2019.2934228.

Qu, S., Xu, W., Zhao, J. and Zhang, H. (2021), "Design and implementation of a fast sliding-mode speed controller with disturbance compensation for SPMSM syste", *IEEE T. Transp. Electrificat.* http://doi.org/10.1109/TTE.2021.3060102.

Rahimi, A., Alibeigloo, A. and Safarpour, M. (2020), "Three-dimensional static and free vibration analysis of graphene platelet–reinforced porous composite cylindrical shell", *J. Vib. Control.*, 26(19-20), 1627-1645. http://doi.org/10.1177/1077546320902340.

Razavian, L., Naghipour, M., Shariati, M. and Safa, M. (2020), "Experimental study of the behavior of composite timber columns confined with hollow rectangular steel sections under compression", *Struct. Eng. Mech.*, **74**(1), 145-156. https://doi.org/10.12989/sem.2020.74.1.145.

Rizk-Allah, R.M., Hassanien, A.E. and Elhoseny, M. (2018), "A multi-objective transportation model under neutrosophic environment", *Comput. Electr. Eng.*, **69**, 705-719. http://doi.org/10.1016/j.compeleceng.2018.02.024.

Safa, M., Sari, P.A., Shariati, M., Suhatril, M., Trung, N.T., Wakil, K. and Khorami, M. (2020), "Development of neuro-fuzzy and neuro-bee predictive models for prediction of the safety factor of eco-protection slopes", *Physica A*, **550**, 124046. http://doi.org/10.1016/j.physa.2019.124046.

Safarpour, H., Pourghader, J. and Habibi, M. (2019), "Influence of spring-mass systems on frequency behavior and critical voltage of a high-speed rotating cantilever cylindrical three-dimensional shell coupled with piezoelectric actuator", *J. Vib. Control.*, **25**(9), 1543-1557. http://doi.org/10.1177/1077546319828465.

Safarpour, M., Ghabussi, A., Ebrahimi, F., Habibi, M. and Safarpour, H. (2020), "Frequency characteristics of FG-GPLRC viscoelastic thick annular plate with the aid of GDQM", *Thin Wall. Struct.*, **150**, 106683. http://doi.org/10.1016/j.tws.2020.106683.

Safarpour, M. and Alibeigloo, A. (2021), "Elasticity solution for bending and frequency behavior of sandwich cylindrical shell with FG-CNTRC face-sheets and polymer core under initial stresses", *Int. J. Appl. Mech.*, **13**(2), 2150020. http://doi.org/10.1142/S1758825121500204.

Salari, F.E.E. (2016), "Thermal loading effects on electro-mechanical vibration behavior of piezoelectrically actuated inhomogeneous size-dependent Timoshenko nanobeams", *Adv. Nano Res.*, **4**(3), 197-228. https://doi.org/10.12989/anr.2016.4.3.197.

Saračević, M., Adamović, S., Maček, N., Elhoseny, M. and Sarhan, S. (2020), "Cryptographic keys exchange model for smart city applications", *IET Intell. Transp. Syst.*, **14**(11), 1456-1464. http://doi.org/ 10.1007/s00542-016-2822-6

Shahgholian-Ghahfarokhi, D., Safarpour, M. and Rahimi, A. (2019), "Torsional buckling analyses of functionally graded porous nanocomposite cylindrical shells reinforced with graphene platelets (GPLs)", *Mech. Based Des. Struct.*, 1-22. http://doi.org/10.1080/15397734.2019.1666723.

Shahverdi, H., Barati, M.R. and Hakimelahi, B. (2019), "Post-buckling analysis of honeycomb core sandwich panels with geometrical imperfection and graphene reinforced nano-composite face sheets", *Mater. Res. Express.*, **6**(9), 095017. http://doi.org/10.1088/2053-1591/ab2b74/meta.

Shankar, K. and Elhoseny, M. (2019), "Trust based cluster head election of secure message transmission in MANET using multi secure protocol with TDES", *J. UCS.* **25**(10), 1221-1239. http://doi.org/ 10.1007/s00339-016-0365-4.

Shankar, K., Elhoseny, M., Lakshmanaprabu, S., Ilayaraja, M., Vidhyavathi, R., Elsoud, M.A. and Alkhambashi, M. (2020), "Optimal feature level fusion based ANFIS classifier for brain MRI image classification", *Cincurr Comp Pract E.*, **32**(1). http://doi.org/ 10.1002/cpe.4887.

Shariati, M., Ramli Sulong, N.H. and Arabnejad Khanouki, M.M. (2010), "Experimental and analytical study on channel shear connectors in light weight aggregate concrete", *Proceedings of the 4th International Conference on Steel & Composite Structures*, Sydney, Australia, July.

Shariati, M., Toghroli, A., Jalali, A. and Ibrahim, Z. (2017), "Assessment of stiffened angle shear connector under monotonic and fully reversed cyclic loading", *Proceedings of Fifth International Conference on Advances in Civil, Structural and Mechanical Engineering-CSM*, New York. U.S.A., September.

Shariati, M., Faegh, S.S., Mehrabi, P., Bahavarnia, S., Zandi, Y., Masoom, D.R., Toghroli, A., Trung, N.-T. and Salih, M.N. (2019), "Numerical study on the structural performance of corrugated low yield point steel plate shear walls with circular openings", *Steel Compos. Struct.*, **33**(4), 569-581. https://doi.org/10.12989/scs.2019.33.4.569.

Shariati, M. (2020), "Evaluation of seismic performance factors for tension-only braced frames", *Steel Compos. Struct.*, **35**(4), 599-609. https://doi.org/10.12989/scs.2020.35.4.599.

Shariati, A., Ghabussi, A., Habibi, M., Safarpour, H., Safarpour, M., Tounsi, A. and Safa, M. (2020a), "Extremely large oscillation and nonlinear frequency of a multi-scale hybrid disk resting on nonlinear elastic foundation", *Thin Wall. Struct.*, **154**, 106840. https://doi.org/10.1016/j.tws.2020.106840.

Shariati, A., Mohammad-Sedighi, H., Żur, K.K., Habibi, M. and Safa, M. (2020b), "Stability and dynamics of viscoelastic moving rayleigh beams with an asymmetrical distribution of material parameters", *Symmetry*, **12**(4), 586. http://doi.org/10.3390/sym12040586.

Shariati, M., Mafipour, M.S., Haido, J.H., Yousif, S.T., Toghroli, A., Trung, N.T. and Shariati, A. (2020c), "Identification of the most influencing parameters on the properties of corroded concrete beams using an Adaptive Neuro-Fuzzy Inference System (ANFIS)", *Steel Compos. Struct.*, **34**(1), 155-171. https://doi.org/10.12989/scs.2020.34.1.155.

Shariati, M., Mafipour, M.S., Mehrabi, P., Ahmadi, M., Wakil, K., Trung, N.T. and Toghroli, A. (2020d), "Prediction of concrete strength in presence of furnace slag and fly ash using hybrid ANN-GA (Artificial Neural Network-Genetic Algorithm)", *Smart Struct. Syst.*, **25**(2), 183-195. https://doi.org/10.12989/sss.2020.25.2.183.

Shi, J., Lu, Y. and Zhang, J. (2019), "Approximation attacks on strong PUFs", *IEEE T. Comput. Aid. D.*, **39**(10), 2138-2151. http://doi.org/ 10.1109/TCAD.2019.2962115.

Sobhy, M. (2020), "Differential quadrature method for magneto-hygrothermal bending of functionally graded graphene/Al sandwich-curved beams with honeycomb core via a new higher-order theory", *J. Sandw. Struct. Mater.*, 1099636219900668. https://doi.org/10.1177/1099636219900668.

Suryawanshi, V.J., Pawar, A.C., Palekar, S.P. and Rade, K.A. (2020), "Defect detection of composite honeycomb structure by vibration analysis technique", *Mater. Today Proc.*, **27**, 2731-2735. http://doi.org/ 10.1016/j.matpr.2019.12.192.

Tang, Y. and Elhoseny, M. (2019), "Computer network security evaluation simulation model based on neural netwo", *J. Intell. Fuzzy Syst.*, **37**(3), 3197-3204. http://doi.org/10.3233/JIFS-179121.

Thakur, S., Singh, A.K., Ghrera, S.P. and Elhoseny, M. (2019), "Multi-layer security of medical data through watermarking and chaotic encryption for tele-health applications ", *Multimedia tools and Applications*. **78**(3), 3457-3470. http://doi.org/10.1007/s11042-018-6263-3

Tharwat, A., Mahdi, H., Elhoseny, M. and Hassanien, A.E. (2018), "Recognizing human activity in mobile crowdsensing environment using optimized k-NN algorithm", *Expert Syst. Appl.*, **107** 32-44. http://doi.org/10.1016/j.eswa.2018.04.017.

Tounsi, A., Benguediab, S., Semmah, A. and Zidour, M. (2013), "Nonlocal effects on thermal buckling properties of double-walled carbon nanotubes", *Adv. Nano Res.*, **1**(1), 1-11, https://doi.org/10.12989/anr.2013.1.1.001.

Tran, T.T., Tran, V.K., Le, P.B., Phung, V.M., Do, V.T. and Nguyen, H.N. (2020), "Forced vibration analysis of laminated composite shells reinforced with graphene nanoplatelets using finite element method", *Adv. Civil Eng.*, **2020** https://doi.org/10.1155/2020/1471037.

Uthayakumar, J., Elhoseny, M. and Shankar, K. (2020), "Highly reliable and low-complexity image compression scheme using neighborhood correlation sequence algorithm in WSN", *IEEE T. Reliab.*, **69**(4), 1398-1423. http://doi.org/10.1109/TR.2020.2972567.

Valayapalayam Kittusamy, S.R., Elhoseny, M. and Kathiresan, S. (2019), "An enhanced whale optimization algorithm for vehicular communication networks", *Int. J. Commun. Syst.*, e3953. http://doi.org/10.1002/dac.3953.

Wang, H., Zhang, H., Dousti, R. and Safarpour, H. (2021), "Dynamic simulation of moderately thick annular system coupled with shape memory alloy and multi-phase nanocomposite face sheets", *Eng. Comput.*, 1-24 https://doi.org/10.1007/s00366-020-01246-x.

Wang, Y.J., Zhang, Z.J., Xue, X.M. and Zhang, L. (2019), "Free vibration analysis of composite sandwich panels with hierarchical honeycomb sandwich core", *Thin Wall. Struct.*, **145** 106425. http://doi.org/https://doi.org/10.1016/j.tws.2019.106425.

Wang, Y., Zeng, R. and Safarpour, M. (2020), "Vibration analysis of FG-GPLRC annular plate in a thermal environment", *Mech. Based Des. Struct.*, 1-19. http://doi.org/10.1080/15397734.2020.1719508.

White, H. (1992), *Artificial NeuralNnetworks:Aapproximation and Learning Theory*, Blackwell Publishers, New Jersey, U.S.A.

Xu, G.D., Zeng, T., Cheng, S., Wang, X.-h. and Zhang, K. (2019), "Free vibration of composite sandwich beam with graded corrugated lattice core", *Compos. Struct.*, **229**, 111466. http://doi.org/ 10.1016/j.compstruct.2019.111466.

Xu, S., Wang, J., Shou, W., Ngo, T., Sadick, A.M. and Wang, X. (2020), "Computer vision techniques in construction: A critical review", *Arch. Comput. Method E.*, 1-15 https://doi.org/10.1007/s11831-020-09504-3.

Xu, X., Cao, D., Zhou, Y. and Gao, J. (2020), "Application of neural network algorithm in fault diagnosis of mechanical intelligence", *Mech. Syst. Signal Pr.*, **141**, 106625. http://doi.org/10.1016/j.ymssp.2020.106625

Xue, X., Zhang, K., Tan, K.C., Feng, L., Wang, J., Chen, G., Zhao, X., Zhang, L. and Yao, J. (2020), "Affine transformation-enhanced multifactorial optimization for heterogeneous problems", *IEEE T. Cybernet.*, http://doi.org/10.1109/TCYB.2020.3036393.

Yang, Y., Hou, C., Lang, Y., Sakamoto, T., He, Y. and Xiang, W. (2019), "Omnidirectional motion classification with monostatic radar system using micro-Doppler signature", *IEEE T. Geosci. Remote.*, **58**(5), 3574-3587. http://doi.org/10.1109/TGRS.2019.2958178.

Yu, Z., Amin, S.U., Alhussein, M. and Lv, Z. (2021), "Research on disease prediction based on improved DeepFM and IoMT", *IEEE Access*, **9**, 39043-39054. http://doi.org/10.1109/ACCESS.2021.3062687.

Yuan, X., Li, D., Mohapatra, D. and Elhoseny, M. (2018), "Automatic removal of complex shadows from indoor videos using transfer learning and dynamic thresholding", *Comput. Electr. Eng.*, **70**, 813-825. http://doi.org/10.1016/j.compeleceng.2017.12.026.

Zaher, M., Shehab, A., Elhoseny, M. and Farahat, F.F. (2020), "Unsupervised model for detecting plagiarism in internet-based handwritten Arabic documents", *J. Org. End User Comput. (JOEUC)*. **32**(2), 42-66. http://doi.org/10.4018/JOEUC.2020040103.

Zhang, Z.J., Han, B., Zhang, Q.C. and Jin, F. (2017), "Free vibration analysis of sandwich beams with honeycomb-corrugation hybrid cores", *Compos. Struct.*, **171**, 335-344. http://doi.org/ 10.1016/j.compstruct.2017.03.045.

Zhang, X., Wang, Y., Wang, C., Su, C.Y., Li, Z. and Chen, X. (2018), "Adaptive estimated inverse output-feedback quantized control for piezoelectric positioning stage", *IEEE T. Cybernet.*, **49**(6), 2106-2118. http://doi.org/10.1109/TCYB.2018.2826519.

Zhang, J. and Qu, G. (2019), "Physical unclonable function-based key sharing via machine learning for IoT security", *IEEE T. Ind. Electron.*, **67**(8), 7025-7033. http://doi.org/10.1109/TIE.2019.2938462.

Zhang, Y. and Li, Y. (2019), "Nonlinear dynamic analysis of a double curvature honeycomb sandwich shell with simply supported boundaries by the homotopy analysis method", *Compos. Struct.*, **221**, 110884. http://doi.org/10.1016/j.compstruct.2019.04.056.

Zhang, J. and Shen, C. (2020), "Set-based obfuscation for strong PUFs against machine learning attacks", *IEEE T. Circuit Syst. I*, **68**(1), 288-300. http://doi.org/ 10.1109/TCSI.2020.3028508.

Zhang, J., Chen, Q., Sun, J., Tian, L. and Zuo, C. (2020a), "On a universal solution to the transport-of-intensity equation", *Opt. Lett.*, **45**(13), 3649-3652. http://doi.org/10.1364/OL.391823.

Zhang, J., Sun, J., Chen, Q. and Zuo, C. (2020b), "Resolution analysis in a lens-free on-chip digital holographic microscope ", *IEEE T. Computat. Image*, **6**, 697-710. https://doi.org/10.1109/TCI.2020.2964247.

Zhang, J., Wu, W., Li, C., Yang, M., Zhang, Y., Jia, D., Hou, Y., Li, R., Cao, H. and Ali, H.M. (2020c), "Convective heat transfer coefficient model under nanofluid minimum quantity lubrication coupled with cryogenic air grinding Ti–6Al–4V", *Int. J. Precision Eng. Manuf. Green Technol.*. 1-23. http://doi.org/10.1007/s40684-020-00268-6.

Zhang, P., Ge, Z. and Safarpour, M. (2020d), "Size-dependent dynamic stability analysis of the cantilevered curved Microtubule-associated proteins (MAPs)", *J. Biomol. Struct. Dyn.*, 1-13. http://doi.org/10.1080/07391102.2020.1758211.

Zhang, X., Shamsodin, M., Wang, H., NoormohammadiArani, O., khan, A.M., Habibi, M. and Al-Furjan, M. (2020e), "Dynamic information of the time-dependent tobullian biomolecular structure using a high-accuracy size-dependent theory", *J. Biomol. Struct. Dyn.*, 1-26. http://doi.org/10.1080/07391102.2020.1760939.

Zhang, J., Shen, C., Su, H., Arafin, M.T. and Qu, G. (2021a), "Voltage over-scaling-based lightweight authentication for IoT security", *IEEE T. Comput.*, http://doi.org/10.1109/TC.2021.3049543.

Zhang, K., Zhang, J., Ma, X., Yao, C., Zhang, L., Yang, Y., Wang, J., Yao, J. and Zhao, H. (2021b), "History matching of naturally fractured reservoirs using a deep sparse autoencoder", *SPE J.*, 1-22. http://doi.org/ 10.2118/205340-PA

Zhang, L., Chen, Z., Habibi, M., Ghabussi, A. and Alyousef, R. (2021c), "Low-velocity impac, resonance, and frequency responses of FG-GPLRC viscoelastic doubly curved panel", *Compos. Struct.*, 114000. http://doi.org/10.1016/j.compstruct.2021.114000.

Zhang, L., Zheng, H., Wan, T., Shi, D., Lyu, L. and Cai, G. (2021d), "An integrated control algorithm of power distribution for islanded microgrid based on improved virtual synchronous generator", *IET Renew. Power Gener.*, http://doi.org/10.1049/rpg2.12191.

Zhao, Y., Moradi, Z., Davoudi, M. and Zhuang, J. (2021), "Bending and stress responses of the hybrid axisymmetric system via state-space method and 3D-elasticity theory", *Eng. Comput.*, 1-23. http://doi.org/ 10.1007/s00366-020-01242-1.

Zhou, M., Wang, Y., Liu, Y. and Tian, Z. (2019), "An information-theoretic view of WLAN localization error bound in GPS-denied environment", *IEEE T. Veh. Technol.*, **68**(4), 4089-4093. http://doi.org/10.1109/TVT.2019.2896482.

Zhou, M., Li, X., Wang, Y., Li, S., Ding, Y. and Nie, W. (2020), "6G multi-source information fusion based indoor positioning via Gaussian kernel density estimation", *IEEE Internet Thing J.*, http://doi.org/10.1109/JIOT.2020.3031639.

Zhou, M., Li, Y., Tahir, M.J., Geng, X., Wang, Y. and He, W. (2021), "Integrated statistical test of signal distributions and access point contributions for Wi-Fi indoor localization", *IEEE T. Veh. Technol.*, http://doi.org/10.1109/TVT.2021.3076269.

Zuo, C., Chen, Q., Tian, L., Waller, L. and Asundi, A. (2015), "Transport of intensity phase retrieval and computational imaging for partially coherent fields: The phase space perspective", *Opt. Laser Eng.*, **71**, 20-32. https://doi.org/10.1016/j.optlaseng.2015.03.006.

Zuo, C., Sun, J., Li, J., Zhang, J., Asundi, A. and Chen, Q. (2017), "High-resolution transport-of-intensity quantitative phase microscopy with annular illumination", *Scientific Report*, **7**(1), 1-22. https://doi.org/10.1038/s41598-017-06837-1.